Closed string self-energy on the lightcone worldsheet lattice

Georgios Papathanasiou and Charles B. Thorn

Phys. Rev. D **86**, 066002 — Published 5 September 2012

DOI: 10.1103/PhysRevD.86.066002

Closed String Self-energy on the Lightcone Worldsheet Lattice [1]

Georgios Papathanasiou[2] and Charles B. Thorn[3]

Institute for Fundamental Theory
Department of Physics, University of Florida, Gainesville FL 32611
(July 6, 2012)

Abstract

We study the one loop correction to the closed bosonic string propagator, including the possibile presence of D-branes, by discretizing the light cone worldsheet on an $M \times N$ rectangular lattice, with $M \propto P^+$ and $N + 1 \propto ix^+$. The integrals over the moduli then become sums which we evaluate numerically. The main purpose of this study is to assess the reliability of the worldsheet lattice as a regulator of the divergences in string perturbation theory. There are two natural geometrical counterterms for the lightcone worldsheet, one proportional to the area of the worldsheet and the other proportional to the length of worldsheet boundaries, tracing the ends of open strings. We show that the divergences in the closed string self-energy can be cancelled by the area counterterm and a renormalization of the Regge slope parameter. The residual finite part is compatible with Lorentz invariance, provided a novel regularization, natural to the lightcone worldsheet lattice and described in this article, is employed.

[1]Supported in part by the Department of Energy under Grant No. DE-FG02-97ER-41029.
[2]E-mail address: georgios@ufl.edu
[3]E-mail address: thorn@phys.ufl.edu

1 Introduction

String theory has long been known to be a generalization of gauge theory due to the presence of a massless spin one state in the open string spectrum. Since all of the massive states of the theory have masses proportional to $\sqrt{2\pi T_0} = 1/\sqrt{\alpha'}$, the string theory goes over to the gauge theory in the infinite tension limit $\alpha' \to 0$. This, together with the fact that closed strings have a massless spin two state, has inspired the discovery of many deep connections between string theory on the one hand and gauge theory coupled to gravity on the other. The AdS/CFT correspondence [1] which asserts the equivalence of $\mathcal{N} = 4$ supersymmetric gauge theory to type IIB superstring theory on an $AdS_5 \times S^5$ space time manifold is one of the most spectacular of these. Although motivated by the physical properties of open string theory with $\alpha' > 0$, the final conclusion is reached by taking $\alpha' \to 0$. The finiteness (conformal invariance) of the $\mathcal{N} = 4$ theory plays a key role in justifying the $\alpha' \to 0$ limit.

The corresponding hypothesis for an asymptotically free gauge theory like the gluonic sector of QCD is more obscure. However, there is little doubt that string theory can offer important insights into some aspects of QCD. In this article we launch a critical analysis of the possibility that 't Hooft's $N \to \infty$ limit [2] of QCD might be usefully analyzed by replacing it with the sum of open string planar diagrams, keeping $\alpha' > 0$. There are several reasons to hope this helps. First, the organization of multiloop string diagrams is dramatically simpler than the corresponding gauge theory diagrams: there is only one planar open string diagram at each loop order, whereas the number of planar gauge theory diagrams grows exponentially with order. Secondly, the 0 loop open string planar diagrams describe the evolution of a "bare" worldsheet which becomes "dressed" with the inclusion of planar loops. This provides a very natural setting for the description of a confining flux tube which may survive the limit $\alpha' \to 0$. Finally there is the long held expectation that the ultraviolet behavior of gauge theory diagrams will be mitigated by the "stringiness" associated with finite α', making the latter better defined.

We focus on this last point in this article. It is not so much the ultraviolet divergences themselves that concern us here–after all those can be absorbed in coupling renormalization in gauge theories. Rather, it is the extreme care that must be taken in gauge theory to preserve gauge and Lorentz invariance in the finite part that remains after renormalization. Order by order in perturbation theory, this can be accomplished by employing a suitable regularization, the most popular of which is dimensional regularization. But as soon as one aims to extract the consequences of summing all the planar diagrams, especially if one must rely on numerical methods, the soundness of dimensional regularization becomes somewhat questionable. For example the powerful conclusions derived from lattice gauge theory would be much less convincing if they relied on an unphysical regularization such as "analytic continuation" of the dimension of spacetime. It is desirable to have a digitization scheme which can be relied on to give the correct physical results without such an artifice. Thirty five years ago Giles and one of us [3] (GT) proposed a digitization of the sum of planar open string diagrams based on lightcone quantization [4, 5] in its path history formulation [6]. In the present article we set out to assess the reliability of this specific lattice model for perturbative calculations.

Let us briefly review the GT proposal, in order to set the stage for the rest of the paper. In lightcone quantization of the bosonic string [5], one takes $x^+ = (x^0 + x^1)/\sqrt{2}$ as the quantum evolution parameter and labels points on a string by a parameter σ defined so that $P^+ = (P^0 + P^1)/\sqrt{2}$ is uniformly distributed on the string. In effect these two choices eliminate x^+ and x^- as dynamical variables, leaving only the $D-2$ transverse coordinates $\boldsymbol{x}(\sigma)$ as quantum operators. Mandelstam worked out the path history form of this quantization [6] using imaginary time $\tau \equiv ix^+$. Then the propagator for a free string is simply the path integral over the $\boldsymbol{x}(\sigma,\tau)$ where $0 \le \sigma \le P^+$ and $0 \le \tau \le T$ parameterize a rectangular region of dimensions $P^+ \times T$. The path integrand is simply e^{-S}, with S the lightcone Euclidean action

$$S = \frac{1}{2}\int_0^T d\tau \int_0^{P^+} d\sigma(\dot{\boldsymbol{x}}^2 + T_0^2 \boldsymbol{x}'^2). \tag{1}$$

In this language a general open string planar diagram is calculated by integrating this same integrand over a worldsheet with several slits of variable length and location as depicted in Fig 1.

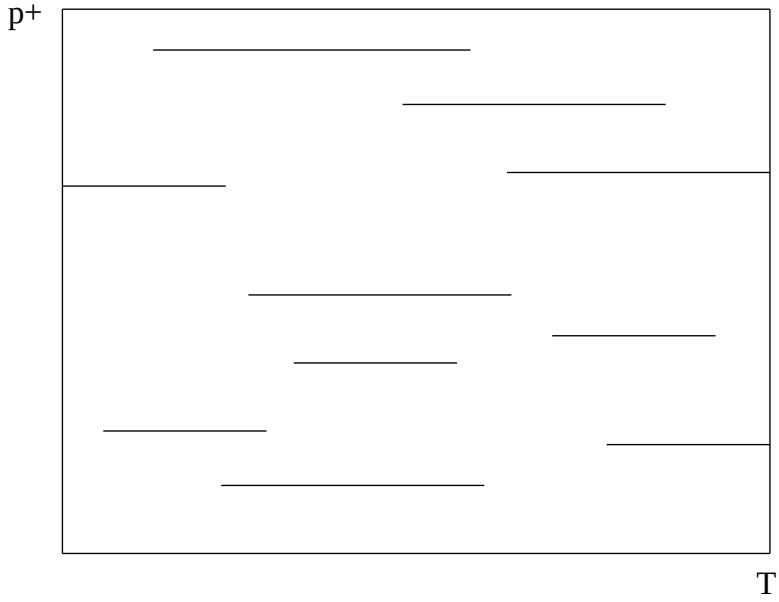

Figure 1: Typical open string planar diagram on the lightcone worldsheet. This one is a seven loop 5 string function

The GT proposal is simply to digitize Mandelstam's interacting string diagrams by defining a rectangular $M \times N$ grid with $T = (N+1)a$ and $P^+ = MaT_0$. Then the integration variables $\boldsymbol{x}(\sigma,\tau) \to \boldsymbol{x}_i{}^j$ and the lattice action is simply

$$S \;\to\; \frac{T_0}{2}\sum_{ij}\left[(x_i{}^{j+1} - x_i{}^j)^2 + (x_{i+1}^j - x_i{}^j)^2\right] \tag{2}$$

A quick look at the lattice corresponding to a multiloop open string diagram Fig. 2, shows that a slit is nothing but a row of missing spatial bonds (links), and summing over all planar diagrams is simply summing over all patterns of missing spatial bonds. One can

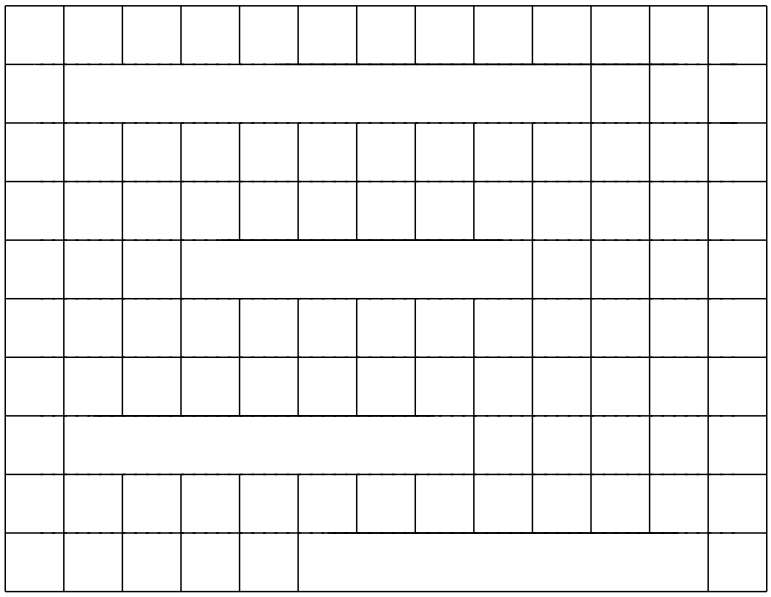

Figure 2: Multiloop lattice worldsheet: each loop is a row of missing links.

easily incorporate the sum over missing bond patterns into the lattice sum over histories by introducing an Ising-like variable ${S_i}^j = 0, 1$ on each spatial link. Then the worldsheet action describing the sum of all open string planar diagrams is simply

$$\begin{aligned} S_{\rm Planar} &= \frac{T_0}{2}\sum_{ij}\left[({x_i}^{j+1}-{x_i}^j)^2+{S_i}^j(x_{i+1}^j-{x_i}^j)^2\right] \\ &\qquad -\sum_{ij}\left[{S_i}^j(1-{S_i}^{j+1})+{S_i}^{j+1}(1-{S_i}^j)\right]\ln g \end{aligned} \tag{3}$$

The purpose of the $\ln g$ term is to insert a factor of g at the beginning and end of each row of missing bonds. Then, in addition to integrating each ${x_i}^j$ from $-\infty$ to $+\infty$, one sums each ${S_i}^j$ over the values 0 and 1 to obtain the sum over all planar diagrams.

If no further adjustments were necessary, we could study this system numerically, e.g. through Monte Carlo simulation. By analyzing the large N behavior of the path integral, one could read off spectral information by identifying exponential behaviors $e^{-aE_\lambda(M)N}$, where $E_\lambda(M)$ are the eigenvalues of P^-. On general grounds we should expect the large M behavior

$$E_\lambda(M) \;\sim\; \alpha M+\beta+\frac{\gamma_\lambda}{M}+\cdots \tag{4}$$

The αM term is a bulk worldsheet effect and the β term is associated with boundaries. The coefficients α, β depend on the details of the lattice model and violate the requirement that

$2P^-P^+ - \boldsymbol{p}^2 = m_\lambda^2$ is a Lorentz invariant. Fortunately there are two geometrical counterterms naturally associated with the worldsheet path integral: one proportional to the area of the worldsheet and another proportional to the length of worldsheet boundaries. Thus the Lorentz violating terms noted above can always be cancelled. As noted in [3] the area term is dynamically inconsequential for the sum of diagrams because the slits representing loops have zero area, so that the area term is identical for all diagrams contributing to the same process. The boundary term depends on the number and lengths of the slits. It can be thought of as an energy cost assigned to the disappearance of a bond. In the Ising spin description of the sum over loops it is represented by a term $(D-2)B\sum_{ij}(1-S_i{}^j)$ added to S. The boundary term is absent for closed strings, but is required for a Lorentz invariant *free* open string spectrum. This is because the Gaussian lattice worldsheet path integral implies an open string zero point energy

$$aP^-(M) \;=\; (D-2)\sum_{m=1}^{M-1}\sinh^{-1}\sin\frac{m\pi}{2M} \sim (D-2)\left[\frac{2G}{\pi}M + B - \frac{1}{2}\sinh^{-1}1 - \frac{\pi}{24M}\right] \quad (5)$$

as $M\to\infty$, where G is Catalan's constant. Cancelling the second term requires $B\to B_0 = (1/2)\sinh^{-1}(1)$ for $g=0$. Since the β term in the energy will in general depend on g, we can't know the value of B at finite g *a priori*, so in practice it must be left as a free counterterm parameter to be determined by requiring that the final answer be consistent with Lorentz invariance.

More generally, we can regard B as a free parameter of the lattice model, which we don't necessarily have to insist is Lorentz covariant. Taking B large enough lifts the P^- of any multi-open string intermediate state above all the $g=0$ closed string energy eigenstates that survive the continuum limit[4]. Then the severe infrared divergences in loop diagrams caused by the open string tachyons are removed, making the multi-loop expansion well defined, albeit with a loss of Lorentz covariance. For numerical studies we should therefore calculate for general B large enough to remove instabilities; and only at the end of the calculation would we scan for a value of B which restores Lorentz covariance, if possible.

But there is no *a priori* guarantee that these two counterterms can remove all Lorentz violating artifacts from this lattice worldsheet construction. For instance, the authors of [7] developed a lightcone worldsheet formalism which mapped the planar diagrams of gauge theories in lightcone gauge to a worldsheet system with exactly the features of the open string planar diagrams just described. String coordinates were employed, but their dynamics were topological in the sense that all but a single zero mode decoupled in the path history sum. In this way the worldsheet diagrams were designed to yield precisely the "bare" Feynman diagrams of the gauge theory. Digitization of this worldsheet in the manner of GT amounted to a scheme for cutting off the UV and IR divergences of these Feynman diagrams. To test the reliability of this cutoff, the authors of [8] calculated the one loop diagrams contributing to the scattering of glue by glue regulated by the GT worldsheet lattice. They found that the artificial divergences associated with lightcone quantization could indeed be absorbed in the

[4]In effect with B this large one imposes confinement on the free theory! The crucial issue is then whether or not confinement survives as B is reduced to a value that restores Lorentz invariance.

bulk or boundary worldsheet counterterms. Further the divergences associated with charge renormalization (asymptotic freedom) had the correct coefficients. Unfortunately, this was not the end of the story. There remained gauge violating terms that could only be cancelled by: (1) a divergent gluon self mass, (2) a finite wave function renormalization, (3) a finite adjustment to the three gluon function, and (4) a finite constant adjustment to the 4 gluon function. Indeed these are precisely the adjustments generally required when a physical cutoff is employed in loop calculations [9]. All of these adjustments, being polynomials in the external momenta, are consistent with locality. The bottom line is that the lightcone worldsheet lattice as a regulator of gauge theory diagrams is no better than other physical cutoffs. Unfortunately this means that we should expect the necessary counterterms to proliferate with the inclusion of multiloop diagrams.

In this paper we begin to explore whether the GT lattice does a reliable (or at least better) job regulating open string planar diagrams than it does with field theory planar diagrams. Does keeping $\alpha' > 0$ control the proliferation of counterterms? Is it possible that the bulk and boundary counterterms will be sufficient by themselves? We start with the simplest self energy diagram: the one loop correction to the closed string propagators. This process involves only a single intermediate open string state and hence has the singularity structure of a tree diagram. Since the corrections to the open string propagator involve complications associated with the multi-string intermediate sates and worldsheet boundaries, we choose to defer the open string analysis to a subsequent paper, and we restrict our attention here to the corrections to the closed string propagator.

Because of the tree structure of the closed string self-energy diagrams, the sum over K, the number of time steps that the intermediate open string exists, converges for both the closed string tachyon and graviton, even with $B = B_0$. Nonetheless the calculations of Sections 3 and 5 (with $B = B_0$) will establish Lorentz violations in both the tachyon and graviton. Fortunately, these Lorentz violations disappear if the calculations are done holding $B > B_0$, taking $B \to B_0$ only at the end of the calculation. In any case, this is the only way to make sense of multi-loop diagrams, so we don't think its necessity at one loop is a drawback.

The article is organized as follows. In Section 2 we obtain explicit formulas for the one loop energy shifts of the closed string ground state (tachyon) and the closed string graviton state. Each term in the K summand involves determinants of $M \times M$ overlap matrices. These formulas are evaluated and analyzed with the help of `Mathematica` in Section 3[5]. In Section 4 we extend the formulas to include open strings ending on Dp-branes, and similarly perform their numerical evaluation in Section 5. In this case, instead of an energy shift, the one loop correction gives the amplitude for a closed string scattering off the Dp-brane. Additional discussion is given in the concluding Section 6. Several appendices collect a number of technical results, including normal mode expansions, determinant formulas, and overlap matrices, that are useful for the discussion in the main text. We also include additional evidence for the robustness of our numerical results.

[5]For the interested reader, we provide the evaluation code and a sample of our analysis in a `Mathematica` file accompanying the source format of this article on the arXiv.

2 Closed String Self-Energy

Before calculating the self-energy diagram on the lattice, we briefly recall the known expression for the continuum self-energy. In the language of conformal field theory we need the amplitude with two closed string vertex operators, say at say 1 and ∞ on the complex plane from which a disk of radius $q < 1$ has been excised. Consulting for example [10], we find the result for the closed string tachyon self-energy:

$$-\Delta P^- = \frac{C}{2P^+}\int_0^1 \frac{dq}{q^3}(1-q^2)^2 \tag{6}$$

which is obviously seriously divergent at $q = 0$: there are quadratic and logarithmic divergences in the q integration. To get further insight into the fate of these divergences, we do the path integral in lightcone parameterization, using the conformal transformation methods of [11, 12]. The (still seriously divergent) result in D spacetime dimensions is

$$-\Delta P^- = C' P^+ \int_0^\infty dT \left[\frac{2\pi}{P^+ \sinh(\pi T T_0/P^+)}\right]^{(D-2)/8} \tag{7}$$

where T is the length of the slit on the lightcone Mandelstam diagram, which is the total ix^+ over which the intermediate open string propagates. The factor of P^+ is just the result of integrating the σ independent integrand over vertical location of the slit $0 < \sigma < P^+$. When $D = 26$ this expression reduces to (6) which can be seen with the change of integration variable

$$q = \frac{1 - e^{-\pi T T_0/P^+}}{1 + e^{-\pi T T_0/P^+}}. \tag{8}$$

We can get a rough idea of what we should get from the lattice calculation by simply discretizing $T = aK$ and $P^+ = aMT_0$. Then the discretization of (7) reads:

$$-a\Delta P^- = \left(C' T_0^{-1/4}(aT_0)^{(26-D)/8}\right) M \sum_{K=1}^{\infty} \left[\frac{2\pi}{M \sinh(\pi K/M)}\right]^{(D-2)/8} \tag{9}$$

Of course discretizing the result of a continuum calculation is not the same as doing the discretized calculation from the beginning, but it at least can serve to guide the eye. For example one feature we immediately see from (9) is that the quadratic divergence seen in (6) is expected to be reflected in the lattice calculation as a linear term in M in P^-, which can be absorbed in the bulk counterterm described in the introduction. We turn next to the actual lattice calculation of the self-energy.

We start with the expression for the summand of the one loop correction to the closed string propagator, depicted in Fig. 3. It is a product of factors, one for each of the $D-2$ transverse coordinates $\boldsymbol{x}_i^j$. In the following we will display only 1 of the factors, calling its

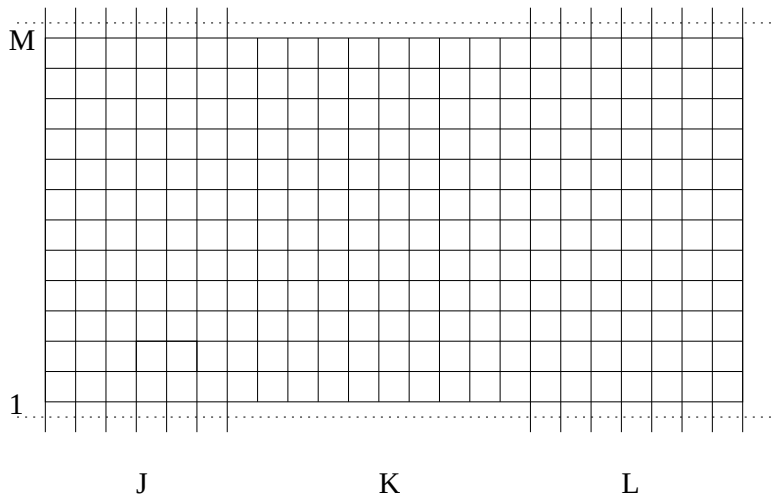

Figure 3: Lattice worldsheet for the closed string self-energy. The dotted lines are identified. There are $K-1$ missing links.

coordinate x_i^j:

$$\begin{aligned}\langle N+1,\{x^f\}|0,\{x^i\}\rangle^{closed}(K,J) &= \int dx_i^K dx_i^L \langle L,\{x^f\}|0,\{x^L\}\rangle^{closed}\langle K,\{x^L\}|0,\{x^K\}\rangle^{open} \\ &\quad \langle J,\{x^K\}|0,\{x^i\}\rangle^{closed} e^{-T_0[(x_M^L-x_1^L)^2+(x_M^K-x_1^K)^2]/4} \qquad (10)\\ &= \mathcal{D}^{closed}(J)\mathcal{D}^{open}(K)\mathcal{D}^{closed}(L)\int dx_i^K dx_i^L e^{iW-(K-1)B_0-T_0[(x_M^L-x_1^L)^2+(x_M^K-x_1^K)^2]/4}\end{aligned}$$

where $J+K+L=N+1$, and $B_0=(1/2)\sinh^{-1}1$ is the counter term which removes the boundary contribution to the free open string P^-. Regarding the intermediate open string as a closed string with a row of missing links, we see that $K-1$ is the number of missing links, which we have taken to be the ones linking site 1 to site M. The open and closed string free propagators are defined in Appendix C. The factors $\mathcal{D}$, which are the corresponding propagators for vanishing values for the initial and final coordinates, are related to determinants of the worldsheet discretized Laplacian, and are defined in Appendix B.

Energy eigenvalues are determined by identifying exponential time ($\tau=ix^+$) dependence in the closed string propagator $e^{-P^-\tau}\to e^{-a(N+1)P^-}$. In perturbation theory $P^-=P_0^-+\Delta P^-$ and

$$e^{-a(N+1)P^-} = e^{-a(N+1)P_0^-}\left[1-a(N+1)\Delta P^-+\cdots\right] \qquad (11)$$

so we identify $-a\Delta P^-$ as the coefficient of $N+1$ in the one loop correction to the closed string propagator. The factor $N+1$ is associated with one of the sums over the creation and destruction times of the intermediate open string. In practice the factor is removed by using time translation invariance to fix, say, the creation time, and summing only over the destruction time.

If we desire to use this formalism to calculate the corrections to excited energy levels, it is necessary to deal with the fact that then the summand over K grows exponentially with K. A convenient approach is to add a term $-K\epsilon$ to the exponent, which can be thought of as adding ϵ to B_0. Since all of the physically meaningful excited states have an excitation energy of order $1/M$, as long as $\epsilon > 0$ is independent of M this is enough to tame the exponential divergence. Actually, since B_0 is a necessary counterterm which is expected to receive corrections in perturbation theory, we cannot know *a priori* what its value should be. All we know is $B = (1/2)\sinh^{-1} 1 + \mathcal{O}(g^2)$. Thus in the context of nonperturbative studies of the worldsheet path integral, it should be taken as a parameter to be tuned at the end of the calculation to ensure Lorentz covariance.

For some states, such as the ground state and graviton state, the absence of lower energy open string states that couple means that the K sum converges without the need for ϵ. However, as we shall see later, because the convergence is then only like $e^{-K/M}$, ultraviolet divergences become entangled with infrared divergences, which then leads to violations of Lorentz invariance since $M \propto P^+$. Introducing an $\epsilon > 0$ prevents these artifacts from entering. Thus, we should keep $\epsilon > 0$ even in those fortuitous cases where it isn't strictly necessary for convergence.

2.1 Correction to the Closed String Ground Energy

Since there is only one ground state, it is uniquely singled out by taking $J, L \to \infty$, in which case it suffices to simplify matters by setting $x^i = x^f = 0$. Then iW is simplified to

$$\begin{aligned} iW &= -\frac{T_0}{2}\Big[q_0^{K2}\left(\frac{1}{J}+\frac{1}{K}\right) + q_0^{L2}\left(\frac{1}{K}+\frac{1}{L}\right) - 2q_0^L q_0^K \frac{1}{K} \\ &\quad + \sum_m (q_{cm}^{K2} + q_{sm}^{K2}) \sinh\lambda_m^c \coth J\lambda_m^c + \sum_m (q_{cm}^{L2} + q_{sm}^{L2}) \sinh\lambda_m^c \coth L\lambda_m^c \\ &\quad + \sum_m (q_{om}^{L2} + q_{om}^{K2}) \sinh\lambda_m^o \coth K\lambda_m^o - 2\sum_m q_{om}^L q_{om}^K \frac{\sinh\lambda_m^o}{\sinh K\lambda_m^o}\Big] \end{aligned} \tag{12}$$

In this equation $\lambda_m^o = 2\sinh^{-1}\sin(m\pi/2M)$ and $\lambda_m^c = 2\sinh^{-1}\sin(m\pi/M)$ are the discrete time versions of the normal mode frequencies for the open and closed strings,respectively. Correspondingly, the q's are the normal mode coordinates of the open or closed string, defined in Appendix A. Note that when it makes no essential difference, we shall restrict M to be odd to keep the description of the closed string modes as simple as possible.

We change integration variables to the closed string normal mode coordinates q_0, q_{cm}, q_{sm} for both K and L. The Jacobian for this variable change is unity, and we can express the q_{om} in terms of the closed string modes as follows:

$$q_{om} = \begin{cases} q_{cm/2} & m \text{ even} \\ \frac{2}{M}\sum_{m'=1}^{(M-1)/2} q_{sm'} U_{mm'} & m \text{ odd} \end{cases} \tag{13}$$

where the overlap matrix $U_{mm'}$ is defined in Appendix D. We also need

$$x_M - x_1 \;=\; -2\sqrt{\frac{2}{M}}\sum_{m'=1}^{(M-1)/2} q_{sm'}\sin\frac{m'\pi}{M} \tag{14}$$

Then

$$\begin{aligned}
iW - \frac{T_0}{4}\left[(x_M^L - x_1^L)^2 + (x_M^K - x_1^K)^2\right] = \\
-\frac{T_0}{2}\Bigg[q_0^{K2}\left(\frac{1}{J}+\frac{1}{K}\right) + q_0^{L2}\left(\frac{1}{K}+\frac{1}{L}\right) - 2q_0^L q_0^K\frac{1}{K} \\
+\sum_m q_{cm}^{K2}\sinh\lambda_m^c(\coth J\lambda_m^c + \coth K\lambda_m^c) + \sum_m q_{cm}^{L2}\sinh\lambda_m^c(\coth L\lambda_m^c + \coth K\lambda_m^c) \\
-2\sum_m q_{cm}^L q_{cm}^K\frac{\sinh\lambda_m^c}{\sinh K\lambda_m^c} + \sum_m q_{sm}^{K2}\sinh\lambda_m^c\coth J\lambda_m^c + \sum_m q_{sm}^{L2}\sinh\lambda_m^c\coth L\lambda_m^c \\
+\sum_{m\ \mathrm{odd}}(q_{om}^{L2}+q_{om}^{K2})\sinh\lambda_m^o\coth K\lambda_m^o - 2\sum_{m\ \mathrm{odd}} q_{om}^L q_{om}^K\frac{\sinh\lambda_m^o}{\sinh K\lambda_m^o} \\
+\frac{4}{M}\sum_{m',m''}(q_{sm'}^K q_{sm''}^K + q_{sm'}^L q_{sm''}^L)\sin\frac{m'\pi}{M}\sin\frac{m''\pi}{M}\Bigg]
\end{aligned} \tag{15}$$

Because of the equality $q_{o2m} = q_{cm}$, the integration over q_0 and the q_{cm} precisely implements closure on these modes. This means that the result of those integrations is just the contribution of those modes to $\mathcal{D}^{closed}(N+1)$. Consulting Appendix B for the various $\mathcal{D}$'s, the outcome of the integration over q_0 and the q_{cm} can be written

$$\begin{aligned}
&\langle N+1,\{x^f\}|0,\{x^i\}\rangle^{closed} \\
&\quad= \mathcal{D}_{\cos}^{\mathrm{closed}}(N+1)\mathcal{D}_{\sin}^{closed}(J)\mathcal{D}_{\mathrm{odd}}^{open}(K)\mathcal{D}_{\sin}^{closed}(L)\int dq_{sm}^K dq_{sm}^L e^{iW'-(K-1)B_0} \\
&\quad= \mathcal{D}^{\mathrm{closed}}(N+1)\frac{\mathcal{D}_{\sin}^{closed}(J)\mathcal{D}_{\mathrm{odd}}^{open}(K)\mathcal{D}_{\sin}^{closed}(L)}{\mathcal{D}_{\sin}^{closed}(N+1)}\int dq_{sm}^K dq_{sm}^L e^{iW'-(K-1)B_0}
\end{aligned} \tag{16}$$

$$\begin{aligned}
iW' = -\frac{T_0}{2}\Bigg[\sum_m(q_{sm}^{K2})\sinh\lambda_m^c\coth J\lambda_m^c + \sum_m(q_{sm}^{L2})\sinh\lambda_m^c\coth L\lambda_m^c \\
+\sum_{m',m''}(q_{sm'}^K q_{sm''}^K + q_{sm'}^L q_{sm''}^L)\Big(\frac{4}{M^2}\sum_{m\ \mathrm{odd}} U_{mm'}U_{mm''}\sinh\lambda_m^o\coth K\lambda_m^o \\
+\frac{4}{M}\sin\frac{m'\pi}{M}\sin\frac{m''\pi}{M}\Big) - \frac{8}{M^2}\sum_{m',m''} q_{sm'}^K q_{sm''}^L\sum_{m\ \mathrm{odd}} U_{mm'}U_{mm''}\frac{\sinh\lambda_m^o}{\sinh K\lambda_m^o}\Bigg]
\end{aligned} \tag{17}$$

and we remind the reader that there are $D-2$ such factors. To isolate the shift in a specific energy level, we need to identify the exponential behavior in J, L as they approach infinity.

For the ground state energy shift, it is sufficient to directly take $J, L \to \infty$ with K fixed. Then the $\coth J, \coth L \to 1$ and

$$\mathcal{D}_{\rm sin}^{\rm closed}(N+1) \;\to\; e^{-(N+1)\sum_{m=1}^{(M-1)/2}\lambda_m^c/2}\left(\frac{T_0}{2\pi}\right)^{(M-1)/4}\prod_{m=1}^{(M-1)/2}\sqrt{2\sinh\lambda_m^c} \tag{18}$$

$$\frac{\mathcal{D}_{\rm sin}^{\rm closed}(J)\mathcal{D}_{\rm sin}^{\rm closed}(L)}{\mathcal{D}_{\rm sin}^{\rm closed}(N+1)} \;\to\; e^{K\sum_{m=1}^{(M-1)/2}\lambda_m^c/2}\left(\frac{T_0}{2\pi}\right)^{(M-1)/4}\prod_{m=1}^{(M-1)/2}\sqrt{2\sinh\lambda_m^c} \tag{19}$$

Change integration variables to $\bar{q}_m = q_{sm}\sqrt{(T_0/\pi)\sinh\lambda_m^c}$. And we have

$$\begin{aligned}
&\langle N+1,\{x^f\}|0,\{x^i\}\rangle^{closed} \\
&\quad\to \mathcal{D}^{\rm closed}(N+1)\frac{\mathcal{D}_{\rm odd}^{open}(K)e^{K\sum_{m=1}^{(M-1)/2}\lambda_m^c/2}}{\prod_m\sqrt{(T_0/\pi)\sinh\lambda_m^c}}\int d\bar{q}_m^K d\bar{q}_m^L e^{iW''-(K-1)B_0} \\
&\quad\to \mathcal{D}^{\rm closed}(N+1)\frac{e^{K\sum_{m=1}^{M-1}(\lambda_m^c-\lambda_m^o)/2}}{\prod_{m=1,\rm odd}^{M-1}\sqrt{1-e^{-2K\lambda_m^o}}}\prod_{m=1}^{M-1}\sqrt{\frac{\sinh\lambda_m^o}{\sinh\lambda_m^c}}\int d\bar{q}_m^K d\bar{q}_m^L e^{iW''-(K-1)B_0}
\end{aligned} \tag{20}$$

where iW'' is defined below. It can be shown that

$$\begin{aligned}
\prod_{m=1}^{M-1}\sinh\lambda_m^o &= 2^{-(M-1)}\sqrt{M\frac{\sinh 2M\sinh^{-1}1}{\sinh 2\sinh^{-1}1}} \\
&= 2^{-(M-1)}\sqrt{M\frac{\sinh M\sinh^{-1}1\cosh M\sinh^{-1}1}{\sqrt{2}}}
\end{aligned} \tag{21}$$

$$\prod_{m=1}^{M-1}\sinh\lambda_m^c = 2^{-(M-1)}M\sinh M\sinh^{-1}1 \tag{22}$$

so, restoring all $D-2$ factors in the amplitude and summing only over K, the time interval spanned by the open string propagator, we infer

$$\begin{aligned}
-a\Delta P^-_{G,closed} &= M\sum_K\left[\frac{\langle N+1,(0)\}|0,\{0\}\rangle^{closed}}{\mathcal{D}^{\rm closed}(N+1)}\right]^{D-2} \\
&= M\sum_{K=1}^{\infty}\left[\frac{e^{K\sum_{m=1}^{M-1}(\lambda_m^c-\lambda_m^o)/2-(K-1)B_0}}{\prod_{m=1,odd}^{M-1}\sqrt{1-e^{-2K\lambda_m^o}}}\left(\frac{\coth M\sinh^{-1}1}{M\sqrt{2}}\right)^{1/4}\int d\bar{q}_m^K d\bar{q}_m^L e^{iW''}\right]^{D-2}
\end{aligned} \tag{23}$$

$$\begin{aligned}
iW'' &= -\frac{\pi}{2}\Big[\sum_m(\bar{q}_m^{K2}+\bar{q}_m^{L2}) + \sum_{m',m''}\frac{\bar{q}_{m'}^K\bar{q}_{m''}^K+\bar{q}_{m'}^L\bar{q}_{m''}^L}{\sqrt{\sinh\lambda_{m'}^c\sinh\lambda_{m''}^c}} \\
&\qquad\Big(\frac{4}{M^2}\sum_{m\ \rm odd}U_{mm'}U_{mm''}\sinh\lambda_m^o\coth K\lambda_m^o + \frac{4}{M}\sin\frac{m'\pi}{M}\sin\frac{m''\pi}{M}\Big)
\end{aligned}$$

$$-\frac{8}{M^2}\sum_{m',m''}\frac{\bar{q}^K_{sm'}\bar{q}^L_{sm''}}{\sqrt{\sinh\lambda^c_{m'}\sinh\lambda^c_{m''}}}\sum_{m\ \text{odd}}U_{mm'}U_{mm''}\frac{\sinh\lambda^o_m}{\sinh K\lambda^o_m}\Big]$$

$$\equiv\ -\pi\left[\sum_{m',m''}(\bar{q}^K_{m'}\bar{q}^K_{m''}+\bar{q}^L_{m'}\bar{q}^L_{m''})A_{m'm''}+2\sum_{m',m''}\bar{q}^K_{m'}\bar{q}^L_{m''}B_{m'm''}\right] \tag{24}$$

With the definitions on the last line

$$\int d\bar{q}^K_m d\bar{q}^L_m e^{iW''}\ =\ \det{}^{-1/2}\begin{pmatrix}A & B\\ B & A\end{pmatrix}=\det{}^{-1/2}(A+B)\ \det{}^{-1/2}(A-B). \tag{25}$$

The last equality follows because the eigenvectors of $\begin{pmatrix}A & B\\ B & A\end{pmatrix}$ can be taken to be of the form $\begin{pmatrix}v_\pm\\ \pm v_\pm\end{pmatrix}$ where $v_\pm$ is an eigenvector of $A\pm B$. Finally we summarize the result

$$-a\Delta P^-_{G,closed}\ =$$

$$M\sum_{K=1}^{\infty}\left[\left(\frac{\coth M\sinh^{-1}1}{M\sqrt{2}}\right)^{1/4}\frac{e^{K\sum_{m=1}^{M-1}(\lambda^c_m-\lambda^o_m)/2-(K-1)B_0}}{\prod_{m=1,odd}^{M-1}\sqrt{1-e^{-2K\lambda^o_m}}}\det{}^{-1/2}\begin{pmatrix}A & B\\ B & A\end{pmatrix}\right]^{D-2} \tag{26}$$

$$A_{m'm''}\ =\ \frac{\delta_{m'm''}}{2}+\frac{2}{M}\frac{\sin(m'\pi/M)\sin(m''\pi/M)}{\sqrt{\sinh\lambda^c_{m'}\sinh\lambda^c_{m''}}}$$
$$+\frac{2}{M^2}\sum_{m\ \text{odd}}\frac{U_{mm'}U_{mm''}\sinh\lambda^o_m\coth K\lambda^o_m}{\sqrt{\sinh\lambda^c_{m'}\sinh\lambda^c_{m''}}} \tag{27}$$

$$B_{m'm''}\ =\ -\frac{2}{M^2}\sum_{m\ \text{odd}}\frac{U_{mm'}U_{mm''}\sinh\lambda^o_m}{\sqrt{\sinh\lambda^c_{m'}\sinh\lambda^c_{m''}}\sinh K\lambda^o_m} \tag{28}$$

$$(A\pm B)_{m'm''}\ =\ \frac{\delta_{m'm''}}{2}+\frac{2}{M}\frac{\sin(m'\pi/M)\sin(m''\pi/M)}{\sqrt{\sinh\lambda^c_{m'}\sinh\lambda^c_{m''}}}$$
$$+\frac{2}{M^2}\sum_{m\ \text{odd}}\frac{U_{mm'}U_{mm''}\sinh\lambda^o_m}{\sqrt{\sinh\lambda^c_{m'}\sinh\lambda^c_{m''}}}\left[\tanh\frac{K\lambda^o_m}{2}\right]^{\pm1} \tag{29}$$

2.2 Correction to the Graviton Energy

For the shift in excited energy levels, we need to identify the non-leading exponential behaviors in the free closed string propagator. Since we also want to pick out a specific spin, it is iimportant to work with the complete amplitude, including all $D-2$ factors:

$$\langle N+1,\{q^f\}|0,\{q^i\}\rangle^{closed}_{\text{total}}\ =\ \left[\mathcal{D}^{closed}(N+1)\right]^{D-2}e^{iW^{closed}_{\text{total}}} \tag{30}$$

$$iW^{closed}_{\text{total}}=-\frac{T_0}{2}\left[\frac{(\boldsymbol{q}_{0,N+1}-\boldsymbol{q}_{0,0})^2}{N+1}+\sum_{m=1}^{M-1}\sinh\lambda^c_m\left((\boldsymbol{q}^2_{m,N+1}+\boldsymbol{q}^2_{m,0})\coth(N+1)\lambda^c_m\right.\right.$$
$$\left.\left.-\frac{2\boldsymbol{q}_{m,N+1}\cdot\boldsymbol{q}_{m,0}}{\sinh(N+1)\lambda^c_m}\right)\right] \tag{31}$$

where $\boldsymbol{q}$ denotes a $D-2$ dimensional vector. Here we identify the $m < M/2$ modes with cosine modes and the $m > M/2$ modes with sine modes. The graviton state on the lattice has energy $2\lambda_1^c$ above the ground state energy, and involves only the 1 modes. Also since it is a symmetric traceless $O(D-2)$ tensor, its contribution to the closed string propagator resides in the second order term in the expansion of

$$\begin{aligned}\exp\left[\frac{T_0(\boldsymbol{q}^c_{1,N+1}\cdot\boldsymbol{q}^c_{1,0}+\boldsymbol{q}^s_{1,N+1}\cdot\boldsymbol{q}^s_{1,0})\sinh\lambda_1^c}{\sinh(N+1)\lambda_1^c}\right] \;\sim\\ 1+2T_0(\boldsymbol{q}^c_{1,N+1}\cdot\boldsymbol{q}^c_{1,0}+\boldsymbol{q}^s_{1,N+1}\cdot\boldsymbol{q}^s_{1,0})\sinh\lambda_1^c e^{-(N+1)\lambda_1^c}\\ +2T_0^2(\boldsymbol{q}^c_{1,N+1}\cdot\boldsymbol{q}^c_{1,0}+\boldsymbol{q}^s_{1,N+1}\cdot\boldsymbol{q}^s_{1,0})^2\sinh^2\lambda_1^c e^{-2(N+1)\lambda_1^c}\end{aligned} \tag{32}$$

as $N+1\to\infty$. The first term (the 1) propagates an $O(D-2)$ scalar, the second term propagates an $O(D-2)$ vector, and the third term propagates a combination of a traceless symmetric tensor, and antisymmetric tensor and a scalar. Since all closed string states must be cyclically invariant, the second (vector) term is projected out of the spectrum. But, in any case, for the shift in the graviton energy, we may simply drop the first two terms, and keep only the symmetric traceless, cyclically invariant part of the third term.

To identify the contribution of the cyclically symmetric states to the third term we consider the new coordinates

$$\boldsymbol{q}_1^\pm \;\equiv\; \boldsymbol{q}_1^c \pm i\boldsymbol{q}_1^s \tag{33}$$

which acquire the factor $e^{\pm 2\pi i/M}$ under a cyclic transformation of one step. To make a cyclically invariant combination, we must have equal numbers of $+$ and $-$ factors:

$$\begin{aligned}\boldsymbol{q}^c_{1,N+1}\cdot\boldsymbol{q}^c_{1,0}+\boldsymbol{q}^s_{1,N+1}\cdot\boldsymbol{q}^s_{1,0} &= \frac{1}{2}(\boldsymbol{q}^+_{1,N+1}\cdot\boldsymbol{q}^-_{1,0}+\boldsymbol{q}^-_{1,N+1}\cdot\boldsymbol{q}^+_{1,0}) \qquad (34)\\ (\boldsymbol{q}^c_{1,N+1}\cdot\boldsymbol{q}^c_{1,0}+\boldsymbol{q}^s_{1,N+1}\cdot\boldsymbol{q}^s_{1,0})^2 &= \frac{1}{4}[(\boldsymbol{q}^+_{1,N+1}\cdot\boldsymbol{q}^-_{1,0})^2+(\boldsymbol{q}^-_{1,N+1}\cdot\boldsymbol{q}^+_{1,0})^2]\\ &\quad+\frac{1}{2}\boldsymbol{q}^+_{1,N+1}\cdot\boldsymbol{q}^-_{1,0}\;\boldsymbol{q}^-_{1,N+1}\cdot\boldsymbol{q}^+_{1,0}\\ &\to \frac{1}{2}\boldsymbol{q}^+_{1,N+1}\cdot\boldsymbol{q}^-_{1,0}\;\boldsymbol{q}^-_{1,N+1}\cdot\boldsymbol{q}^+_{1,0}=\frac{1}{2}q^{+k}_{1,N+1}q^{-l}_{1,N+1}\;q^{-k}_{1,0}q^{+l}_{1,0}\end{aligned}$$

where the last line shows the only contribution that survives the cyclic symmetry requirements. To see the $SO(D-2)$ content write

$$q^{-k}_{1,0}q^{+l}_{1,0} \;=\; q^{ck}_{1,0}q^{cl}_{1,0}+q^{sk}_{1,0}q^{sl}_{1,0}+i(q^{ck}_{1,0}q^{sl}_{1,0}-q^{sk}_{1,0}q^{sk}_{1,0}) \tag{35}$$

The third (imaginary) term gives the contribution of the anti-symmetric tensor, whereas the first two (real) terms give a symmetric tensor, which can further be decomposed into a traceless symmetric tensor and a scalar:

$$q^{ck}_{1,0}q^{cl}_{1,0}+q^{sk}_{1,0}q^{sl}_{1,0}=\left[q^{ck}_{1,0}q^{cl}_{1,0}+q^{sk}_{1,0}q^{sl}_{1,0}-\frac{\delta_{kl}}{D-2}(\boldsymbol{q}^{c2}_{1,0}+\boldsymbol{q}^{s2}_{1,0})\right]+\frac{\delta_{kl}}{D-2}(\boldsymbol{q}^{c2}_{1,0}+\boldsymbol{q}^{s2}_{1,0}) \tag{36}$$

The quantity in square brackets on the right represents the contribution of the graviton in all spin configurations. To identify the graviton energy shift it is sufficient to simply pick one polarization with $k \neq l$ so that the trace subtraction drops out.

$$\left[\exp\left\{\frac{T_0(\boldsymbol{q}^c_{1,N+1}\cdot\boldsymbol{q}^c_{1,0}+\boldsymbol{q}^s_{1,N+1}\cdot\boldsymbol{q}^s_{1,0})\sinh\lambda^c_1}{\sinh(N+1)\lambda^c_1}\right\}\right]_{cyc\ inv} \sim$$

$$1+T_0^2 q^{+k}_{1,N+1}q^{-l}_{1,N+1}\ q^{-k}_{1,0}q^{+l}_{1,0}\sinh^2\lambda^c_1 e^{-2(N+1)\lambda^c_1}+\cdots \quad (37)$$

$$=1+T_0^2(q^{ck}_{1,N+1}q^{cl}_{1,N+1}+q^{sk}_{1,N+1}q^{sl}_{1,N+1})(q^{ck}_{1,0}q^{cl}_{1,0}+q^{sk}_{1,0}q^{sl}_{1,0})\sinh^2\lambda^c_1 e^{-2(N+1)\lambda^c_1} \quad (38)$$

$$+(q^{ck}_{1,N+1}q^{sl}_{1,N+1}-q^{sk}_{1,N+1}q^{cl}_{1,N+1})(q^{ck}_{1,0}q^{sl}_{1,0}-q^{sk}_{1,0}q^{cl}_{1,0})\sinh^2\lambda^c_1 e^{-2(N+1)\lambda^c_1}+\cdots \quad (39)$$

The first 1 term can be dropped in the calculation of the graviton and also the anti-symmetric tensor energy shifts, since it contributes only for scalar states (the tachyonic ground state and the massless dilaton. Then we can take $J, L \to \infty$ in

$$\begin{aligned}&\langle N+1,\{x^f\}|0,\{x^i\}\rangle^{Graviton}_{\rm total}(K,J)\\ &\sim T_0^4\sinh^4\lambda^c_1\left[\mathcal{D}^{closed}(J)\mathcal{D}^{open}(K)\mathcal{D}^{closed}(L)\right]^{D-2}e^{-2(L+J)\lambda^c_1}\\ &\int dq^K_m dq^L_i[q^{ck}_{f,1}q^{cl}_{f,1}+q^{sk}_{f,1}q^{sl}_{f,1}][q^{ck}_{L,1}q^{cl}_{L,1}+q^{sk}_{L,1}q^{sl}_{L,1}][q^{ck'}_{K,1}q^{cl'}_{K,1}+q^{sk'}_{K,1}q^{sl'}_{K,1}][q^{ck'}_{i,1}q^{cl'}_{i,1}+q^{sk'}_{i,1}q^{sl'}_{i,1}]\\ &\qquad e^{iW_{\rm total}-(K-1)(D-2)B_0-T_0[(\boldsymbol{x}^L_M-\boldsymbol{x}^L_1)^2+(\boldsymbol{x}^K_M-\boldsymbol{x}^K_1)^2]/4} \quad (40)\end{aligned}$$

The sum over K of this expression should be compared to the free closed string propagator for the graviton

$$[\mathcal{D}(N+1)]^{D-2}T_0^2\sinh^2\lambda^c_1 e^{-2(N+1)\lambda^c_1}[q^{ck}_{f,1}q^{cl}_{f,1}+q^{sk}_{f,1}q^{sl}_{f,1}][q^{ck}_{i,1}q^{cl}_{i,1}+q^{sk}_{i,1}q^{sl}_{i,1}] \quad (41)$$

to read off the graviton energy shift:

$$\begin{aligned}&MT_0^2\sinh^2\lambda^c_1\sum_{K=1}^{\infty}\left[\frac{\mathcal{D}^{closed}(J)\mathcal{D}^{open}(K)\mathcal{D}^{closed}(L)}{\mathcal{D}(N+1)}\right]^{D-2}e^{2K\lambda^c_1-(K-1)(D-2)B_0}\\ &\int dq^K_m dq^L_i[q^{ck}_{L,1}q^{cl}_{L,1}+q^{sk}_{L,1}q^{sl}_{L,1}][q^{ck'}_{K,1}q^{cl'}_{K,1}+q^{sk'}_{K,1}q^{sl'}_{K,1}]e^{iW_{\rm total}-T_0[(\boldsymbol{x}^L_M-\boldsymbol{x}^L_1)^2+(\boldsymbol{x}^K_M-\boldsymbol{x}^K_1)^2]/4}\\ &=-\frac{a}{2}(\delta_{kk'}\delta_{ll'}+\delta_{kl'}\delta_{lk'})\Delta P^-_{Graviton}+C\delta_{kl}\delta_{k'l'} \quad (42)\end{aligned}$$

where the C term contributes to the dilaton energy shift. (If $C = 0$ the graviton and dilaton remain degenerate.) Here iW is the same expression (15) that we used in the evaluation of the ground state energy shift. A simple way to isolate the graviton shift is to simply choose index values for which the C term decouples. For example, take $k = k' = 1$ and $l = l' = 2$:

$$\begin{aligned}-a\Delta P^-_{Graviton} \;=\; &2MT_0^2\sinh^2\lambda^c_1\sum_{K=1}^{\infty}\left[\frac{\mathcal{D}^{closed}(J)\mathcal{D}^{open}(K)\mathcal{D}^{closed}(L)}{\mathcal{D}(N+1)}\right]^{D-2}e^{2K\lambda^c_1-(K-1)(D-2)B_0}\\ &\int dq^K_m dq^L_m[q^{c1}_{L,1}q^{c2}_{L,1}+q^{s1}_{L,1}q^{s2}_{L,1}][q^{c1}_{K,1}q^{c2}_{K,1}+q^{s1}_{K,1}q^{s2}_{K,1}]e^{iW_{\rm total}-T_0[(\boldsymbol{x}^L_M-\boldsymbol{x}^L_1)^2+(\boldsymbol{x}^K_M-\boldsymbol{x}^K_1)^2]/4}\end{aligned}$$

$$
\begin{aligned}
&= 2MT_0^2 \sinh^2 \lambda_1^c \sum_{K=1}^{\infty} \left[\frac{\mathcal{D}^{closed}(J)\mathcal{D}^{open}(K)\mathcal{D}^{closed}(L)}{\mathcal{D}(N+1)} \right]^{D-2} e^{2K\lambda_1^c - (K-1)(D-2)B_0} \\
&\int dq_m^K dq_m^L [q_{L,1}^{c1} q_{K,1}^{c1} q_{L,1}^{c2} q_{K,1}^{c2} + q_{L,1}^{s1} q_{K,1}^{s1} q_{L,1}^{s2} q_{K,1}^{s2}] e^{iW_{\rm total} - T_0[(\boldsymbol{x}_M^L - \boldsymbol{x}_1^L)^2 + (\boldsymbol{x}_M^K - \boldsymbol{x}_1^K)^2]/4} \\
&\equiv 2MT_0^2 \sinh^2 \lambda_1^c \sum_{K=1}^{\infty} \left[\frac{\mathcal{D}^{closed}(J)\mathcal{D}^{open}(K)\mathcal{D}^{closed}(L)}{\mathcal{D}(N+1)} \right]^{D-2} e^{2K\lambda_1^c - (K-1)B_0} \\
&(\langle q_{L,1}^{c1} q_{K,1}^{c1} \rangle^2 + \langle q_{L,1}^{s1} q_{K,1}^{s1} \rangle^2) \int dq_m^K dq_m^L e^{iW_{\rm total} - T_0[(\boldsymbol{x}_M^L - \boldsymbol{x}_1^L)^2 + (\boldsymbol{x}_M^K - \boldsymbol{x}_1^K)^2]/4} \qquad (43)
\end{aligned}
$$

where in the second and third forms we take advantage of the fact that the integration is over independent Gaussians, so the language of correlations reflected in the $\langle \cdots \rangle$ notation is appropriate. The correlator of cosine modes is just that of the free closed string and is easily shown to be

$$
\langle q_{L,1}^{c1} q_{K,1}^{c1} \rangle = \frac{\sinh L\lambda_1^c \ \sinh J\lambda_1^c}{T_0 \sinh \lambda_1^c \ \sinh(K+J+L)\lambda_1^c} \to \frac{1}{2T_0 \sinh \lambda_1^c} e^{-K\lambda_1^c} \qquad (44)
$$

in the limit $J, L \to \infty$.

The correlator of sine modes is of course more complicated because they involve the nontrivial overlap of the closed and open string modes.

$$
\langle q_{L,1}^{s1} q_{K,1}^{s1} \rangle = \frac{\pi}{T_0 \sinh \lambda_1^c} \langle \bar{q}_{L,1}^{s1} \bar{q}_{K,1}^{s1} \rangle \qquad (45)
$$

$$
\langle \bar{q}_{L,1}^{s1} \bar{q}_{K,1}^{s1} \rangle = \frac{\int d\bar{q}_{K,m} d\bar{q}_{L,m} \bar{q}_{L,1}^s \bar{q}_{K,1}^s e^{iW''}}{\int d\bar{q}_{K,m} d\bar{q}_{L,m} e^{iW''}} \qquad (46)
$$

Recall that $iW'' = -\pi \bar{q}^T \begin{pmatrix} A & B \\ B & A \end{pmatrix} \bar{q}$ so adding a source term $J^T \bar{q}$, we complete the square to evaluate

$$
\langle e^{J^T \bar{q}} \rangle = \exp\left\{ \frac{1}{4\pi} J^T \begin{pmatrix} A & B \\ B & A \end{pmatrix}^{-1} J \right\} \qquad (47)
$$

With the definition

$$
\begin{pmatrix} A & B \\ B & A \end{pmatrix}^{-1} = \begin{pmatrix} A' & B' \\ B' & A' \end{pmatrix} \qquad (48)
$$

$$
\begin{aligned}
A' &= (A - BA^{-1}B)^{-1} = \frac{1}{2}\left((A+B)^{-1} + (A-B)^{-1} \right) \\
B' &= (B - AB^{-1}A)^{-1} = \frac{1}{2}\left((A+B)^{-1} - (A-B)^{-1} \right), \qquad (49)
\end{aligned}
$$

we then have

$$
\langle q_{L,1}^{s1} q_{K,1}^{s1} \rangle = \frac{1}{2T_0 \sinh \lambda_1^c} B'_{1,1} \qquad (50)
$$

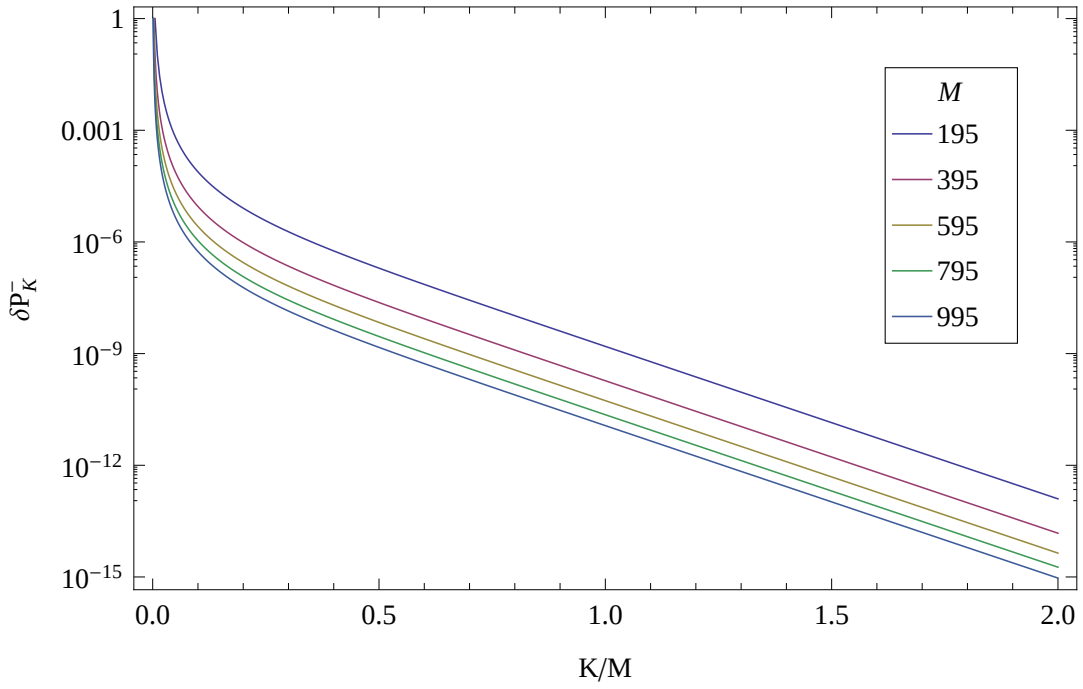

Figure 4: Log-linear plot for the summand of the rescaled ground state energy shift (51), with each curve exhibiting its dependence on K for a fixed value of M. We have rescaled the horizontal axis to K/M in order to demonstrate that for a large enough value of the latter, $\log \delta P_K^-$ develops the same slope. The plot also justifies our choice $K_{max} = 2M$ for the cutoff in the K sum.

3 Numerical Analysis

3.1 Closed String Ground State

Here we will perform a numerical study of the 1-loop shift in the ground state energy for the closed string in $D = 26$ dimensions, with the help of `Mathematica`. In particular, we will rescale the energy shift (26) by an overall factor of M (notice also $\Delta P^-_{G,closed}$ and δP_K^- differ by a minus sign),

$$-\frac{a\Delta P^-_{G,closed}}{M} \equiv \sum_{K=1}^{\infty} \delta P_K^- = \\ = \sum_{K=1}^{\infty} \left[\left(\frac{\coth(M \sinh^{-1} 1)}{M\sqrt{2}} \right)^{1/4} \frac{e^{K \sum_{m=1}^{M-1} (\lambda_m^c - \lambda_m^o)/2 - (K-1)B_0}}{\prod_{m=1,odd}^{M-1} \sqrt{1 - e^{-2K\lambda_m^o}}} \det{}^{-1/2} \begin{pmatrix} A & B \\ B & A \end{pmatrix} \right]^{24} \quad (51)$$

where A and B are given by (27),(28), as it will turn out that this yields a finite quantity for $M \to \infty$, which is just what is expected from the bulk term in ΔP^-. It is instructive to start by investigating the dependence of the summand δP_K^- on M and K, as a means to also set a

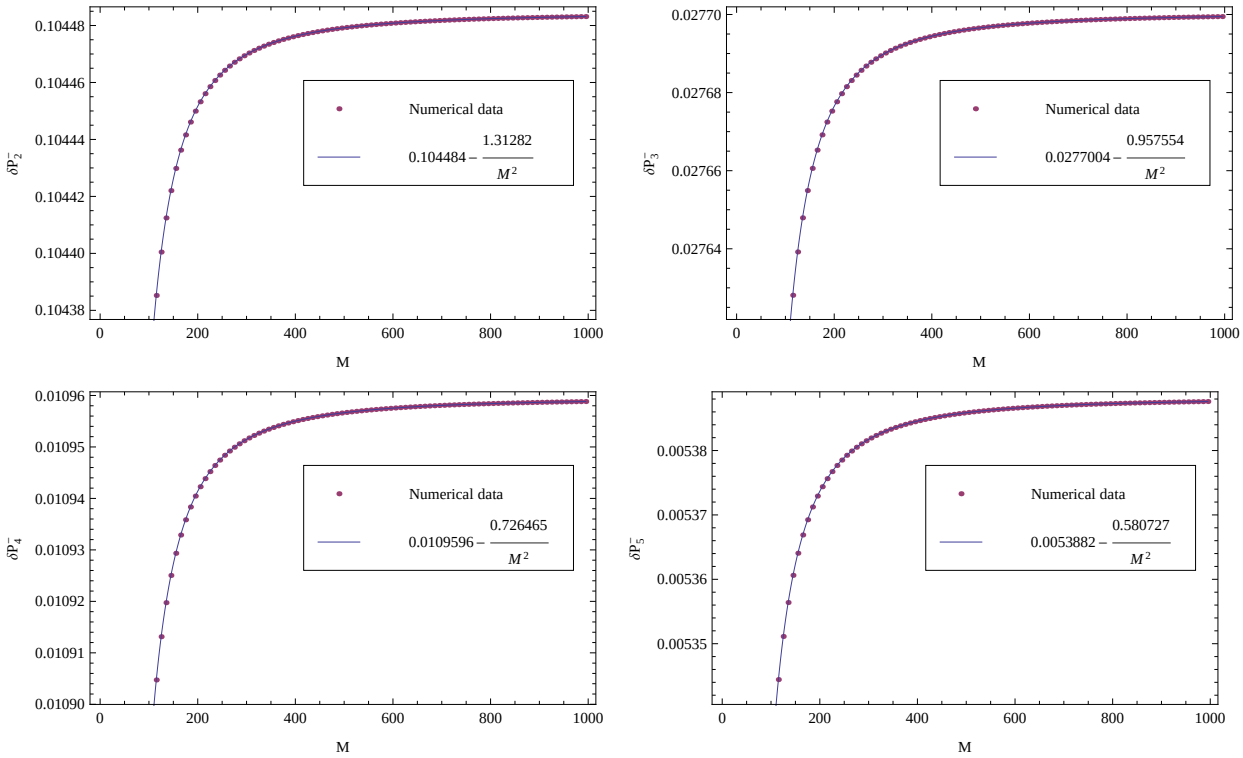

Figure 5: Summand for the rescaled ground state energy shift as a function of M for $K = 2, 3, 4, 5 \ll M$, including fits of the form (52).

reasonable cutoff $K_{max} \geq K$ in the sum. For fixed M, δP_K^- decreases rapidly for increasing K, and for $K \gg M$ it becomes proportional to $e^{-9.428K/M}$ times an M-dependent factor. This fact is evident in figure 4, which also indicates that $K_{max} = 2M$ is a sufficiently large cutoff, given that the largest term in the sum is $\delta P_1^- = 1$ for any M, and $\delta P_{K_{max}} \leq 10^{-12}$ for $M \geq 195$, precisely indicating the accuracy of our cutoff.

For fixed $K \ll M$, we also find a good fit to

$$\delta P_K^- = c_1^K + \frac{c_2^K}{M^2} + \mathcal{O}(\frac{1}{M^3}) \tag{52}$$

where roughly $c_1^K \sim K^{-3}$ and $c_2^K \sim K^{-1}$. The particular examples $K = 2, 3, 4, 5$ are presented in figure 5. Since this behavior changes as K becomes comparable to M, it suggests that the sum over K should give rise to a $\log M/M^2$ term due to

$$\sum_{K=1}^{M} c_2^K \sim H(M) \sim \log M \text{ for } M \gg 1\,, \tag{53}$$

where $H(M)$ is the M-th harmonic number. Similarly the sum of c_1^K yields harmonic numbers of order 3, whose large M expansion suggests the absence of an $1/M$ term.

We should also note that in both regimes we examined, the general structure of the dependence on M and K is correctly captured by the discretized version of the continuum amplitude (9). Denoting the summand of the latter (up to a proportionality factor) with a prime in order to avoid confusion, we have for $D = 26$

$$\delta P_K^{-\prime} = \left(\frac{\pi}{M\sinh(\pi K/M)}\right)^3 = \begin{cases} \left(\frac{2\pi}{M}\right)^3 e^{-3\pi K/M} + \mathcal{O}(e^{-5\pi K/M}) & K \gg M \\ \frac{1}{K^3} - \frac{\pi^2}{2KM^2} + \mathcal{O}(\frac{1}{M^4}) & K \ll M \end{cases} \tag{54}$$

For $K \gg M$ there is also approximate agreement in the value of the exponent, although for the $K \ll M$ expansions more detailed comparison of the coefficients of $\delta P_K^{-\prime}$ and δP_K^- reveals that they are not simply proportional to each other.

Armed with this intuition, we proceed to the numerical calculation of (51), summed up to $K_{max} = 2M$, and for values of M ranging from 5 to 995 in steps of 10. We fit the generated data for different subintervals between $M \in [195, 995]$ to ensure that M is sufficiently large and to test the stability of our fits, and also calculate the value of R^2 as an estimate of their goodness. We find that indeed the fit

$$-\frac{a\Delta P^-_{G,closed}}{M} = c_1 + c_2\frac{1}{M^2} + c_3\frac{\log M}{M^2} \tag{55}$$

with

$$c_1 = 1.158863267 \pm 3\cdot 10^{-9}\,, \quad c_2 = 2.799 \pm 0.011\,, \quad c_3 = -2.800 \pm 0.002 \tag{56}$$

matches excellently with the data, with the values of the coefficients varying only mildly when fitting different subintervals in M (the error estimates are precisely taking this interval dependence into account).

Our main finding of this section, (55), is plotted against the numerical data in figure 6. We've also included the fit with $c_3 = 0$ to show its insufficiency in accurately describing the data. As far as the fit with $c_2 = 0$ is concerned, it leads to values of c_3 which may differ up to 7% depending on the interval of the fit, and generally one should also expect a constant multiplying M inside the logarithm. As additional evidence that the M-dependence is indeed correctly captured by (55), we also mention that when fitting the entire interval $M \in [195, 995]$, the value of R^2 differs from 1 by a mere $3\cdot 10^{-11}$, whereas for the $c_2 = 0$ and $c_3 = 0$ cases the differences are $6\cdot 10^{-5}$ and 0.002 respectively. Finally, our expectations for the absence of an $1/M$ term is confirmed by the fact that its inclusion yields unnaturally small values for its coefficient, and does not substantially improve the fit.

As described in the introduction, the bulk counterterm can be chosen to cancel the contribution to P^- proportional to M, and what is left gives the physically significant contribution. Lorentz invariance requires that this residuum behave at large M as $1/M$, since $\Delta m^2 = 2MaT_0(\Delta P^- - \text{Bulk Term})$. Our results (55),(56) contradict this requirement because of the $\ln M$ dependence. Taken literally, the result implies a logarithmically divergent self mass: $\ln M = \ln P^+/aT_0 = \ln(1/a) + \ln(P^+/T_0)$, which is to be expected from the dq/q behavior in the covariant expression for the self-energy. As is well known this divergence can

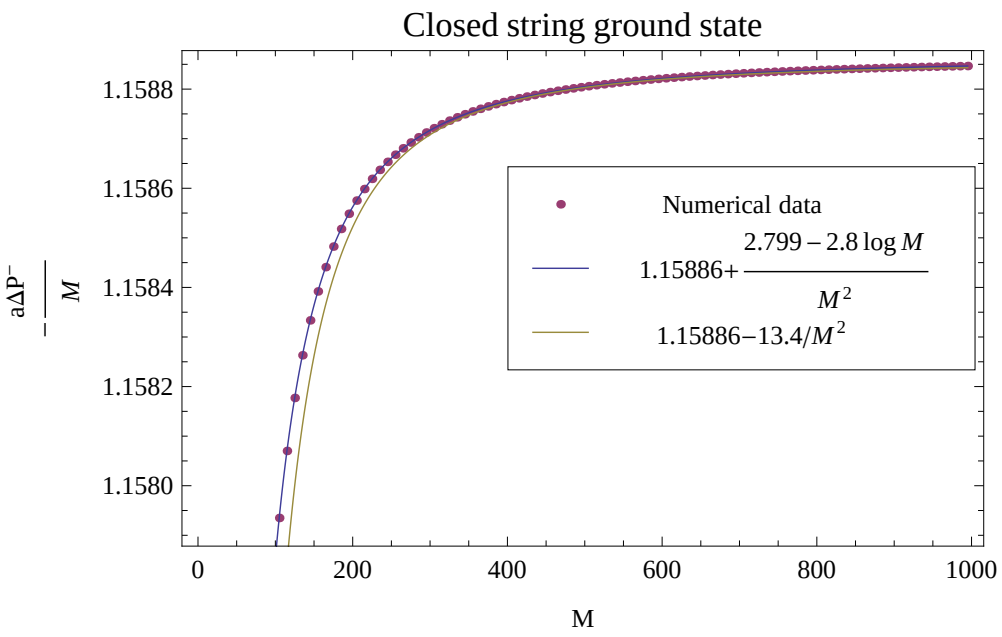

Figure 6: Rescaled ground state energy shift as a function of M. We present fits with and without a $\log M$ term, in order to demonstrate the necessity of the latter for agreement with the data.

be absorbed in a renormalization of the Regge slope parameter $\alpha' = 1/2\pi T_0$. But the $\ln P^+$ signifies a noncovariant finite part.

The origin of this $\ln M$ factor can be traced to the sum over K of the $1/K$ dependence we saw in the summand when $K << M$. The lightcone lattice has cutoff the logarithmic UV divergence (small K), but the large K behavior is cut off at $K = \mathcal{O}(M)$, because the level spacing is of order $1/M$, so $\sum_K (1/K) = \mathcal{O}(\ln M)$. As mentioned in the introduction, the presence of the B_0 counterterm offers a way to interpret the lattice calculation that avoids the difficulty. By adding a small positive constant $B_0 \to B_0 + \epsilon$ the cutoff on the K sum becomes $1/\epsilon$ instead of M, and the residuum will behave as $(1/M)\ln(1/\epsilon)$ which is still divergent as $\epsilon \to 0$, but remains compatible with Lorentz invariance. Then the $\ln(1/\epsilon)$ can be absorbed in a redefinition of T_0 before taking $M \to \infty$. As we shall see in the next subsection, this same interpretation leads to a zero self-energy for the graviton state.

3.2 Graviton

We proceed to investigate how the lightcone lattice handles nontachyonic states by looking at the 1-loop mass shift of the spin-2 excitation of the closed string, representing the graviton. Similarly to the ground state, with the help of (44),(50), we may rewrite (43) in the $J, L \to \infty$

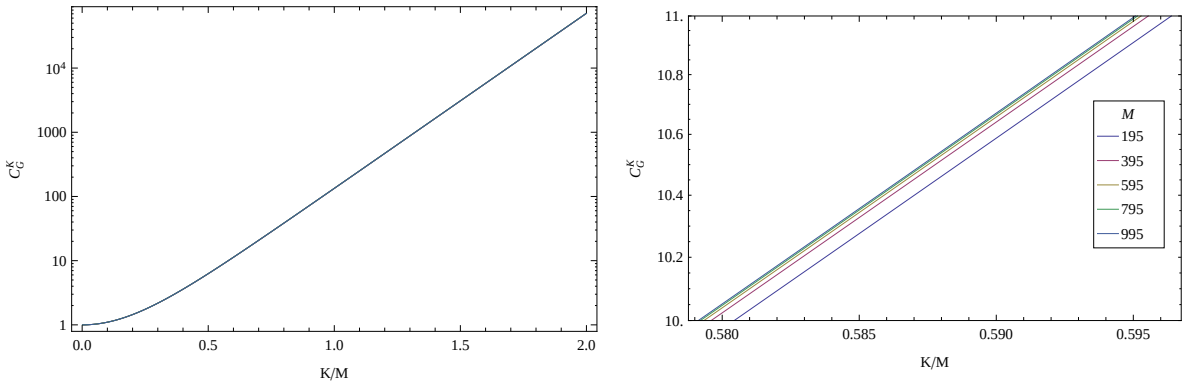

Figure 7: Coefficient C_G^K in the rescaled graviton energy shift (57) as a function of K/M, with each curve corresponding to varying K for a fixed value of M. On the left hand side we plot the entire range of summation for K/M, it is evident that curves for different M values are indistinguishable. On the right hand side we zoom into a small region in order to see the mild dependence of the $\log C_G^K$ offset on M.

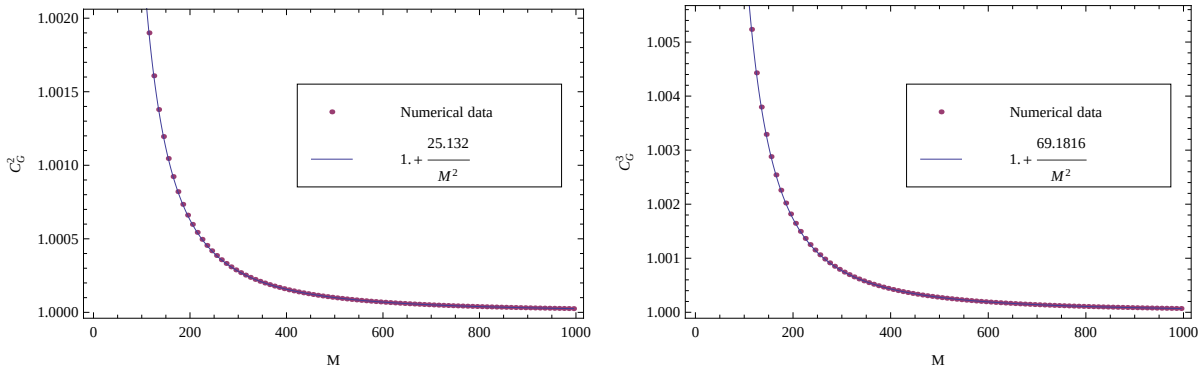

Figure 8: Coefficient C_G^K in the rescaled graviton energy shift (57) as a function M for fixed $K = 2, 3 \ll M$.

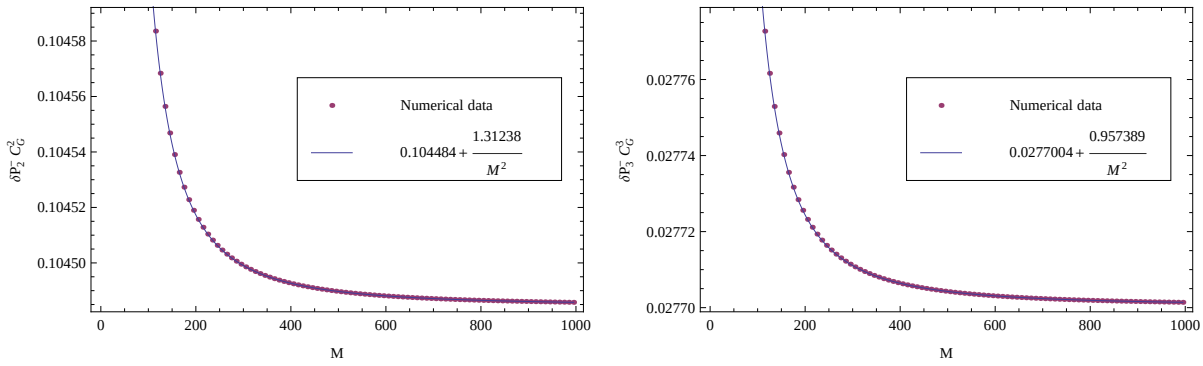

Figure 9: $C_G^K \delta P_K^-$ as a function M for fixed $K = 2, 3 \ll M$. Comparing with figure 5, we notice that the constant terms are equal, and the $1/M^2$ coefficients roughly opposite.

limit as

$$-\frac{a\Delta P^-_{Graviton}}{M} = \frac{1}{2}\sum_{K=1}^{\infty}[1+(e^{K\lambda_1^c}B'_{1,1})^2]\delta P^-_K \equiv \frac{1}{2}\sum_{K=1}^{\infty}(1+C_G^K)\delta P^-_K\,, \tag{57}$$

where δP^-_K is the summand of the rescaled ground state shift, defined in (51).

As δP^-_K has been determined in the previous section, the only additional numerical computation that has to be done is for the coefficient C_G^K. A preliminary analysis shows that for fixed M and varying K this is a rapidly increasing function which for $K \gg M$ becomes proportional to roughly $e^{6.28K/M}$, as can be seen in figure 7. However given the behavior of δP^-_K in the same regime, their product is guaranteed to converge, albeit more slowly. As far as the regime $K \ll M$ is concerned, we observe that $C_G^1 = 1$ for any M, and more generally $C_G^K = 1 + c/M^2 + \mathcal{O}(1/M^3)$. The first two nontrivial examples $K = 2, 3$ are plotted in figure 8. The fact that the constant term is independent of K and equal to one guarantees that the leading divergence for the ground state and the graviton is the same, as it should for all states.

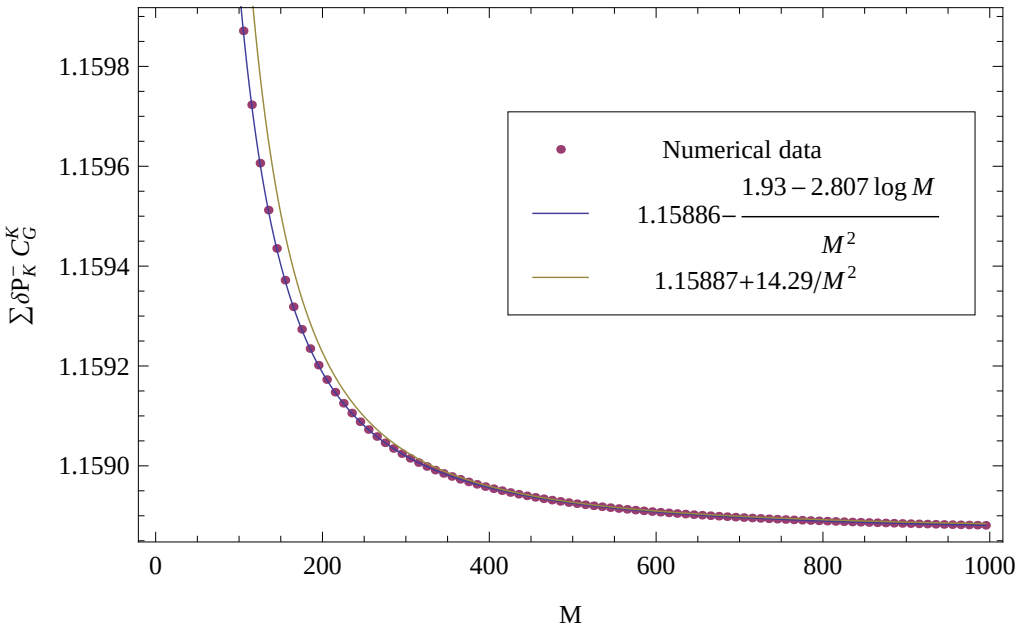

Figure 10: $\sum_K C_G^K \delta P^-_K$ as a function of M. Again fits with and without a $\log M$ term are presented, so as to demonstrate its necessity for matching with the data.

Before evaluating the entire sum (57), it is again useful to examine $C_G^K \delta P^-_K$ for fixed K. As can be seen in figure 9, for individual $K \ll M$ the latter has an expansion in M of the form (52), where c_1^K are roughly equal and c_2^K are roughly opposite between the ground state and the graviton. Then the sum in K is depicted in figure 10 similarly described by a fit of the form (55), where again the coefficients c_1 and c_3 are found to be equal and opposite respectively within our margins of error, however $c_2 = -1.93 \pm 0.04$. This is a first hint that

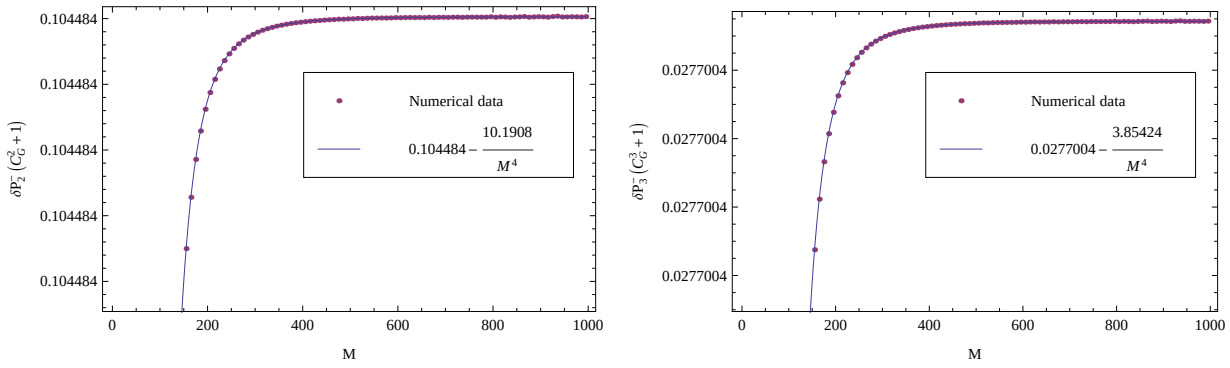

Figure 11: Entire summand of rescaled graviton energy shift (57) as a function M for fixed $K = 2, 3 \ll M$.

although additional cancellations occur for the graviton, which may remove the divergent $\log M$ terms, the lattice regularization, in the absence of the ϵ prescription, still leaves an unphysical finite mass shift for the graviton. Moving now to the entire summand (57), from figure 11 we infer it behaves as

$$\frac{1}{2}(1+C_G^K)\delta P_K^- = \tilde{c}_1^K + \frac{\tilde{c}_2^K}{M^4} + \mathcal{O}(\frac{1}{M^5}) \tag{58}$$

with $\tilde{c}_1^K \simeq c_1^K \sim K^{-3}$ and $\tilde{c}_2^K \sim K$, which is consistent with

$$\sum_{K=1}^{M} \tilde{c}_2^K \sim M^2/2 \text{ for } M \gg 1\,, \tag{59}$$

introducing an additional contribution that changes the c_2 coefficient for the graviton, compared to the ground state. Finally, we find that the fit for the entire rescaled energy shift (see Fig. 12)

$$-\frac{a\Delta P^-_{Graviton}}{M} = \tilde{c}_1 + \tilde{c}_2\frac{1}{M^2}\,, \tag{60}$$

with

$$\tilde{c}_1 = 1.158863276 \pm 1.5\cdot 10^{-8} \quad \tilde{c}_2 = 0.454 \pm 0.004\,, \tag{61}$$

is in very good agreement with the numerical data[6] and our previous quantitative and qualitative observations.

Our results indicate the absence of the $\ln M$ Lorentz violating effect we found for the tachyon[7], but still the K sum with a cutoff of $\mathcal{O}(M)$, leads to the undesirable conclusion that the graviton would gain a (necessarily finite) nonzero mass at one loop order. This is a

[6] In particular when fitting on the range $M \in [195, 995]$, R^2 differs from 1 by 10^{-5}. Including an additional $\log M/M^2$ term yields an unnaturally small coefficient and does not improve R^2 significantly.

[7] A $\ln M$ divergence in the graviton self mass could not be absorbed in the Regge slope parameter because at zeroth order the graviton is massless.

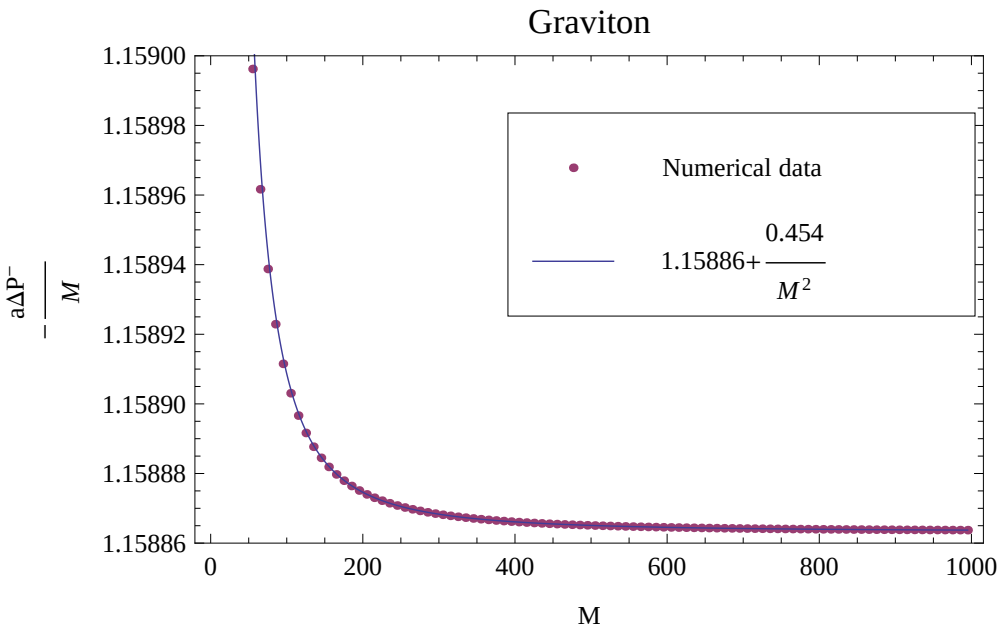

Figure 12: Rescaled graviton energy shift as a function of M.

(more subtle) violation of Lorentz invariance. However, with the ϵ prescription introduced to interpret the tachyon mass shift, this difficulty is avoided. Putting $B_0 \to B_0 + \epsilon$ cuts off the K sum at $\sim 1/\epsilon$, so the large M expansion at fixed ϵ encounters no $1/M^2$ contribution and hence no shift in the graviton mass. It is important to appreciate that this interpretation requires taking the continuum limit *before* taking $\epsilon \to 0$.

4 D-branes

We extend the discussion to the case when several of the transverse open string coordinates satisfy Dirichlet conditions. In current popular terminology this is known as closed string theory in the presence of D-branes [13]. To avoid confusion we will call such coordinates $\boldsymbol{y}_i^j$. We shall follow [14] in adapting the lightcone lattice to Dirichlet boundary conditions. Starting from the closed string potential energy for one such coordinate

$$V_{\text{closed}} \quad = \quad \frac{T_0}{2} \sum_{i=1}^{M} (y_{i+1} - y_i)^2 \tag{62}$$

we pass to the potential energy for a Dirichlet open string with say $y_l = 0$ by the following substitution

$$(y_{l+1} - y_l)^2 + (y_l - y_{l-1})^2 \quad \to \quad y_{l+1}^2 + y_{l-1}^2 + 2\kappa y_l^2. \tag{63}$$

In other words we keep all M degrees of freedom on the lattice. Instead of trying to set $y_l = 0$, we decouple it from the other coordinates and give it a potential $T_0 \kappa y_l^2$ that makes it produce an energy of $\mathcal{O}(1)$ in lattice units. This means that excitations of y_l will have infinite energy in the continuum limit, which therefore locks this degree of freedom in its ground state. The normal modes for the Dirichlet open string coordinates q_{Dm} are defined in Appendix A. In this case it is convenient to alter the corresponding normal mode expansion for the closed string, which for M odd are

$$y_k = \frac{1}{\sqrt{M}} q_0 + \sqrt{\frac{2}{M}} \sum_{m=1}^{(M-1)/2} \left[q_{cm} \cos \frac{2m\pi k}{M} + q_{sm} \sin \frac{2m\pi k}{M} \right]. \tag{64}$$

The modification for M even can be found in Appendix A.

We can express the open string normal modes in terms of the closed string ones

$$q_{\mathrm{D}m} = \begin{cases} q_{sm/2} & \text{for } m \text{ even} \\ \dfrac{2}{M} \displaystyle\sum_{m'=0}^{(M-1)/2} q_{cm'} U^{\mathrm{D}}_{mm'} & \text{for } m \text{ odd} \end{cases} \tag{65}$$

where we have defined $q_{c0} \equiv q_0/\sqrt{2}$, and $U^D_{mm'}$ is given in Appendix D.

In constructing the one loop diagram, we would like the $j = 0, N+1$ sites of the open string propagator be assigned half the closed string potential energy. We have

$$\begin{aligned} V^c - V^{\mathrm{D}} &= \frac{T_0}{2} \left((y_M - y_{M-1})^2 + (y_1 - y_M)^2 - y_1^2 - y_{M-1}^2 - 2\kappa y_M^2 \right) \\ &= -T_0 y_M (y_1 + y_{M-1} + (\kappa - 1) y_M) \equiv -2U(y). \end{aligned} \tag{66}$$

Thus the loop integrand is given by the product of the three propagators times the factor $e^{U(y)}$ at each vertex. In terms of the closed string normal modes

$$y_M = \frac{1}{\sqrt{M}} q_0 + \sqrt{\frac{2}{M}} \sum_{m'=1}^{(M-1)/2} q_{cm'} \equiv \sqrt{\frac{2}{M}} \sum_{m'=0}^{(M-1)/2} q_{cm'} \tag{67}$$

$$\begin{aligned} y_1 + y_{M-1} &= \frac{2}{\sqrt{M}} q_0 + 2\sqrt{\frac{2}{M}} \sum_{m'=1}^{(M-1)/2} q_{cm'} \cos \frac{2m'\pi}{M} \\ &\equiv 2\sqrt{\frac{2}{M}} \sum_{m'=0}^{(M-1)/2} q_{cm'} \cos \frac{2m'\pi}{M} \end{aligned} \tag{68}$$

$$U(y) = \frac{T_0}{M} \sum_{m',m''=0}^{(M-1)/2} q_{cm'} q_{cm''} \left[\kappa - 1 + \cos \frac{2m'\pi}{M} + \cos \frac{2m''\pi}{M} \right] \tag{69}$$

where we defined $q_{c0} \equiv q_0/\sqrt{2}$. Then the one loop correction to the closed string propagator is

$$\sum_K \int dy_i^K dy_i^L e^{-(K-1)B_0^{\mathrm{D}} + U(y^K) + U(y^L)} \langle L, \{y^f\} | 0, \{y^L\} \rangle^{closed} \langle K, \{y^L\} | 0, \{y^K\} \rangle^{\mathrm{D}}$$

$$\langle J, \{y^K\}|0, \{y^i\}\rangle^{closed}$$

$$= \sum_K \mathcal{D}^{closed}(J)\mathcal{D}^{\rm D}(K)\mathcal{D}^{closed}(L)\int dy_i^K dy_i^L e^{iW-(K-1)B_0^{\rm D}+U(y^K)+U(y^L)}$$

where as before we display only one factor for the Dirichlet coordinate y. Note that we expect $B_0^{\rm D} \neq B_0$ because of the different boundary conditions.

4.1 Closed String Tachyon Scattering of D-brane

For the case where $y_i = y_f = 0$ we have, for each Dirichlet coordinate y, a term

$$\begin{aligned} iW + U(y^K) + U(y^L) &= -\frac{T_0}{2}\Bigg[q_0^{K2}\frac{1}{J} + q_0^{L2}\frac{1}{L} \\ &+ \sum_m (q_{cm}^{K2} + q_{sm}^{K2})\sinh\lambda_m^c \coth J\lambda_m^c + \sum_m (q_{cm}^{L2} + q_{sm}^{L2})\sinh\lambda_m^c\coth L\lambda_m^c \\ &+ \sum_m (q_{{\rm D}m}^{L2} + q_{Dm}^{K2})\sinh\lambda_m^{\rm D}\coth K\lambda_m^{\rm D} - 2\sum_m q_{{\rm D}m}^L q_{{\rm D}m}^K \frac{\sinh\lambda_m^{\rm D}}{\sinh K\lambda_m^{\rm D}} \\ &- \frac{2}{M}\sum_{m',m''=0}^{(M-1)/2}\left(q_{cm'}^K q_{cm''}^K + q_{cm'}^L q_{cm''}^L\right)\left(\kappa - 1 + \cos\frac{2m'\pi}{M} + \cos\frac{2m''\pi}{M}\right)\Bigg] \end{aligned}$$

The next step is to change integration variables to the closed string normal modes, $q_0 = q_{c0}\sqrt{2}, q_{cm}, q_{sm}$. The Jacobian for the change of variables $y_k \to q_0, q_{cm}, q_{sm}$ is unity, and further changing $q_0 \to q_{c0}$ gives a factor $\sqrt{2}$. The equality $q_{D2m} = q_{sm}$ means that integrating over the closed string sine modes simply implements closure on these modes. Thus we can write

$$\begin{aligned} &\langle N+1, \{x^f\}|0, \{x^i\}\rangle_{\rm 1loop}^{closed} \\ &\quad = \mathcal{D}_{\rm sin}^{\rm closed}(N+1)\mathcal{D}_{\rm cos}^{closed}(J)\mathcal{D}_{\rm odd}^{\rm D}(K)\mathcal{D}_{\rm cos}^{closed}(L)\int 2dq_{cm}^K dq_{cm}^L e^{iW^{\rm D\prime}-(K-1)B_0^{\rm D}} \\ &\quad = \mathcal{D}^{\rm closed}(N+1)\frac{\mathcal{D}_{\rm cos}^{closed}(J)\mathcal{D}_{\rm odd}^{\rm D}(K)\mathcal{D}_{\rm cos}^{closed}(L)}{\mathcal{D}_{\rm cos}^{closed}(N+1)}\int 2dq_{cm}^K dq_{cm}^L e^{iW^{\rm D\prime}-(K-1)B_0^{\rm D}} \end{aligned} \tag{70}$$

where

$$\begin{aligned} iW^{\rm D\prime} &= -\frac{T_0}{2}\Bigg[q_0^{K2}\frac{1}{J} + q_0^{L2}\frac{1}{L} + \sum_m q_{cm}^{K2}\sinh\lambda_m^c\coth J\lambda_m^c + \sum_m q_{cm}^{L2}\sinh\lambda_m^c\coth L\lambda_m^c \\ &+ \sum_{m=1,{\rm odd}}^{M}(q_{{\rm D}m}^{L2} + q_{{\rm D}m}^{K2})\sinh\lambda_m^{\rm D}\coth K\lambda_m^{\rm D} - 2\sum_{m=1,{\rm odd}}^{M} q_{{\rm D}m}^L q_{{\rm D}m}^K\frac{\sinh\lambda_m^{\rm D}}{\sinh K\lambda_m^{\rm D}} \\ &- \frac{2}{M}\sum_{m',m''=0}^{(M-1)/2}\left(q_{cm'}^K q_{cm''}^K + q_{cm'}^L q_{cm''}^L\right)\left(\kappa - 1 + \cos\frac{2m'\pi}{M} + \cos\frac{2m''\pi}{M}\right)\Bigg] \end{aligned} \tag{71}$$

Taking J, L large, the factors in front of the integral reduce to

$$\begin{aligned}\frac{\mathcal{D}^{closed}_{\rm cos}(J)\mathcal{D}^{\rm D}_{\rm odd}(K)\mathcal{D}^{closed}_{\rm cos}(L)}{\mathcal{D}^{closed}_{\rm cos}(N+1)} &\rightarrow \sqrt{\frac{N+1}{JL}}\frac{e^{K(\sum_{m=1}^{(M-1)/2}\lambda^c_m-\sum_{m,\rm odd}\lambda^{\rm D}_m)/2}}{\prod_{m,odd}\sqrt{1-e^{-2K\lambda^{\rm D}_m}}} \\ &\sqrt{2}\sqrt{\frac{\prod_{m,odd}\sinh\lambda^{\rm D}_m}{\prod_{m=1}^{(M-1)/2}\sinh\lambda^c_m}}\left[\frac{T_0}{2\pi}\prod_{m=1}^{(M-1)/2}\frac{T_0}{\pi}\sinh\lambda^c_m\right] \qquad (72)\end{aligned}$$

Meanwhile

$$\begin{aligned}iW^{\rm D\prime} \rightarrow & -\frac{T_0}{2}\Bigg[\sum_{m'=1}^{(M-1)/2}(q^{K2}_{cm}+q^{L2}_{cm})\sinh\lambda^c_m \\ &+\sum_{m',m''=0}^{(M-1)/2}\left(q^K_{cm'}q^K_{cm''}+q^L_{cm'}q^L_{cm''}\right)\Bigg[\frac{4}{M^2}\sum_{m=1,\rm odd}^{M}U^{\rm D}_{mm'}U^{\rm D}_{mm''}\sinh\lambda^{\rm D}_m\coth K\lambda^{\rm D}_m \\ &-\frac{2}{M}\left(\kappa-1+\cos\frac{2m'\pi}{M}+\cos\frac{2m''\pi}{M}\right)\Bigg] \\ &-\frac{8}{M^2}\sum_{m',m''=0}^{(M-1)/2}q^K_{cm'}q^L_{cm''}\sum_{m=1,\rm odd}^{M}U^{\rm D}_{mm'}U^{\rm D}_{mm''}\frac{\sinh\lambda^{\rm D}_m}{\sinh K\lambda^{\rm D}_m}\Bigg] \qquad (73)\end{aligned}$$

Just as in the Neumann case it is convenient to absorb the factors in square brackets into a rescaling of the integration variables $\bar{q}_m = q_{cm}\sqrt{(T_0/\pi)\sinh\lambda^c_m}$ for $m = 1, \cdots (M-1)/2$ and $\bar{q}_0 = q_0\sqrt{T_0/2\pi} = q_{c0}\sqrt{T_0/\pi}$.

$$\begin{aligned}\frac{\langle N+1,\{x^f\}|0,\{x^i\}\rangle^{closed}_{\rm 1loop}}{\mathcal{D}^{\rm closed}(N+1)} &\sim \sqrt{\frac{2(N+1)}{JL}}\frac{e^{K(\sum_{m=1}^{(M-1)/2}\lambda^c_m-\sum_{m,\rm odd}\lambda^{\rm D}_m)/2-(K-1)B^{\rm D}_0}}{\prod_{m,odd}\sqrt{1-e^{-2K\lambda^{\rm D}_m}}} \\ &\sqrt{\frac{\prod_{m,odd}\sinh\lambda^{\rm D}_m}{\prod_{m=1}^{(M-1)/2}\sinh\lambda^c_m}}\int d\bar{q}^K_m d\bar{q}^L_m e^{iW^{D\prime}} \qquad (74) \\ B^{\rm D}_0 &= B_0-\frac{\lambda^{\rm D}_M}{2} \\ &= \frac{1}{2}\sinh^{-1}1-\sinh^{-1}\sqrt{\frac{\kappa}{2}}=\frac{1}{2}\ln\frac{1+\sqrt{2}}{1+\kappa+\sqrt{\kappa(\kappa+2)}} \qquad (75)\end{aligned}$$

Comparing the prefactors in this formula with the corresponding factors for the Neumann case we see that the extra factors are

$$\sqrt{\frac{2(N+1)}{JL}}\frac{e^{-K\lambda^{\rm D}_M/2}\sqrt{\sinh\lambda^{\rm D}_M}}{\sqrt{1-e^{-2K\lambda^{\rm D}_M}}} \equiv \sqrt{\frac{N+1}{JL}}\sqrt{\eta^{K-1}\frac{1-\eta^2}{1-\eta^{2K}}} \qquad (76)$$

where for brevity we have defined $\eta \equiv 1+\kappa-\sqrt{\kappa(2+\kappa)} \rightarrow 2-\sqrt{3} \approx 0.268$ for $\kappa = 1$. The $\sqrt{(N+1)/JL}$ factor just reflects the fact that the intermediate open string has its ends

fixed in space. In the Neumann case this factor would instead be 1. The factor η^{K-1} can be absorbed in the boundary counterterm, converting its zero coupling value back to B_0. The expansion in powers of η represents excitations of order $\mathcal{O}(1)$ in lattice units, which will be suppressed in the continuum physics.

Finally we turn to the matrix determinant that results from the execution of the Gaussian integration. For this we need to spell out $W^{D\prime}$ which remains after integrating out the closed string sine modes. Expressed in terms of the new variables $\bar{q}_{m'}$, we write

$$iW''_{\rm D} \equiv -\pi\left[\sum_{m',m''}(\bar{q}^K_{m'}\bar{q}^K_{m''}+\bar{q}^L_{m'}\bar{q}^L_{m''})A^{\rm D}_{m'm''}+2\sum_{m',m''}\bar{q}^K_{m'}\bar{q}^L_{m''}B^{\rm D}_{m'm''}\right] \tag{77}$$

$$A^{\rm D}_{00} = \frac{2}{M^2}\sum_{m=1,\rm odd}^{M}U^{\rm D}_{m0}U^{\rm D}_{m0}\sinh\lambda^{\rm D}_m\coth K\lambda^{\rm D}_m-\frac{1+\kappa}{M} \tag{78}$$

$$A^{\rm D}_{0m'}=A^{\rm D}_{m'0} = \frac{2}{M^2}\sum_{m=1,\rm odd}^{M}U^{\rm D}_{mm'}U^{\rm D}_{m0}\frac{\sinh\lambda^{\rm D}_m\coth K\lambda^{\rm D}_m}{\sqrt{\sinh\lambda^c_{m'}}}-\frac{\kappa+\cos 2m'\pi/M}{M\sqrt{\sinh\lambda^c_{m'}}} \tag{79}$$

$$\begin{aligned}A^{\rm D}_{m'm''} &= \frac{\delta_{m'm''}}{2}+\frac{2}{M^2}\sum_{m=1,\rm odd}^{M}U^{\rm D}_{mm'}U^{\rm D}_{mm''}\frac{\sinh\lambda^{\rm D}_m\coth K\lambda^{\rm D}_m}{\sqrt{\sinh\lambda^c_{m'}}\sqrt{\sinh\lambda^c_{m''}}}\\ &\quad-\frac{\kappa-1+\cos(2m'\pi/M)+\cos(2m''\pi/M)}{M\sqrt{\sinh\lambda^c_{m'}}\sqrt{\sinh\lambda^c_{m''}}}\end{aligned} \tag{80}$$

$$B^{\rm D}_{00} = -\frac{2}{M^2}\sum_{m=1,\rm odd}^{M}U^{\rm D}_{m0}U^{\rm D}_{m0}\frac{\sinh\lambda^{\rm D}_m}{\sinh K\lambda^{\rm D}_m} \tag{81}$$

$$B^{\rm D}_{0m'}=B^{\rm D}_{m'0} = -\frac{2}{M^2}\sum_{m=1,\rm odd}^{M}U^{\rm D}_{mm'}U^{\rm D}_{m0}\frac{\sinh\lambda^{\rm D}_m}{\sinh K\lambda^{\rm D}_m\sqrt{\sinh\lambda^c_{m'}}} \tag{82}$$

$$B^{\rm D}_{m'm''} = -\frac{2}{M^2}\sum_{m=1,\rm odd}^{M}U^{\rm D}_{mm'}U^{\rm D}_{mm''}\frac{\sinh\lambda^{\rm D}_m}{\sinh K\lambda^{\rm D}_m\sqrt{\sinh\lambda^c_{m'}}\sqrt{\sinh\lambda^c_{m''}}} \tag{83}$$

For a Dp-brane there are $D-p-1\to 25-p$ coordinates satisfying Dirichlet boundary conditions. Putting everything together we have for the zero energy amplitude for a closed string tachyon scattering off a Dp-brane:

$$\begin{aligned}-a\mathcal{M}_{G,closed} &= M\sum_{K=2}^{\infty}\left[\left(\frac{\coth M\sinh^{-1}1}{M\sqrt{2}}\right)^{1/4}\frac{e^{K\sum_{m=1}^{M-1}(\lambda^c_m-\lambda^o_m)/2-(K-1)B_0}}{\prod_{m=1,odd}^{M-1}\sqrt{1-e^{-2K\lambda^o_m}}}\right]^{24}\\ &\quad\left[\det{}^{-1/2}\begin{pmatrix}A & B\\ B & A\end{pmatrix}\right]^{p-1}\left[\sqrt{\frac{2\pi}{MT_0}}\sqrt{\frac{1-\eta^2}{1-\eta^{2K}}}\,\det{}^{-1/2}\begin{pmatrix}A^{\rm D} & B^{\rm D}\\ B^{\rm D} & A^{\rm D}\end{pmatrix}\right]^{25-p}\end{aligned} \tag{84}$$

$$\eta = 1+\kappa-\sqrt{\kappa(\kappa-1)} \tag{85}$$

where the scattering amplitude is obtained from the one loop correction to the two closed string function by stripping off the factor $\sqrt{MT_0(N+1)/2\pi JL}$ for each Dirichlet dimension,

as explained at the end of Appendix C. The $K = 1$ term is not included in the scattering amplitude since it contributes to the I term of the S-matrix.

4.2 Graviton Scattering off D-brane

Let us take the graviton polarizations to lie within the Dp-brane. Then in parallel to the derivation of (43) we must simply insert the factors

$$2T_0^2 \sinh^2 \lambda_1^c (\langle q_{L,1}^{c1} q_{K,1}^{c1} \rangle^2 + \langle q_{L,1}^{s1} q_{K,1}^{s1} \rangle^2) e^{2K\lambda_1^c} = \frac{1}{2}(1 + (B'_{11} e^{K\lambda_1^c})^2) \tag{86}$$

into the K summand for the closed string tachyon scattering amplitude.

5 Numerics of D-branes

In the case of a closed string tachyon scattering off a Dp-brane, it is convenient to define the quantity

$$r_K = \sqrt{\frac{\det(A+B)\det(A-B)}{M \det(A^D + B^D)\det(A^D - B^D)}}\,, \tag{87}$$

such that the corresponding zero energy amplitude (85) may be rewritten as

$$-\frac{a\mathcal{M}_{G,closed}}{M} = \sum_{K=2}^{\infty} \delta P_K^- \left(\sqrt{\frac{1-\eta^2}{1-\eta^{2K}}} r_K \right)^{25-p}, \tag{88}$$

where δP^- is the summand of the tachyon energy shift (51). For simplicity we have set $T_0 = 2\pi$ and also $\kappa = 1$, as we have checked that varying its value does not substantially change our results.

Hence the ratio r_K essentially encodes the difference between Neumann and Dirichlet boundary conditions, and we find that for $K \gg M$ it falls off exponentially to a value of $\mathcal{O}(1)$ which depends very mildly on M, as can be seen in figure 13. For fixed $K \ll M$ we find that the fit

$$r_K = a_1^K + \frac{a_2^K}{M^2} + \mathcal{O}(\frac{1}{M^3}) \tag{89}$$

matches very well with the data (see figure 14 for indicative values of K), and by further examining the fitted coefficients for different values of K, we infer that they roughly vary as

$$a_1^K \approx 0.724 + \frac{0.115}{K-1}\,, \tag{90}$$

$$a_2^K \approx -0.204 + 0.369K\,, \tag{91}$$

see also figure 15. By factoring out the constant term in a_1^K, which dominates r_K, we can infer that the leading dependence of the entire amplitude (88) on p will be equal to $(0.724\sqrt{1-\eta^2})^{25-p}$ or equivalently 0.697^{25-p}.

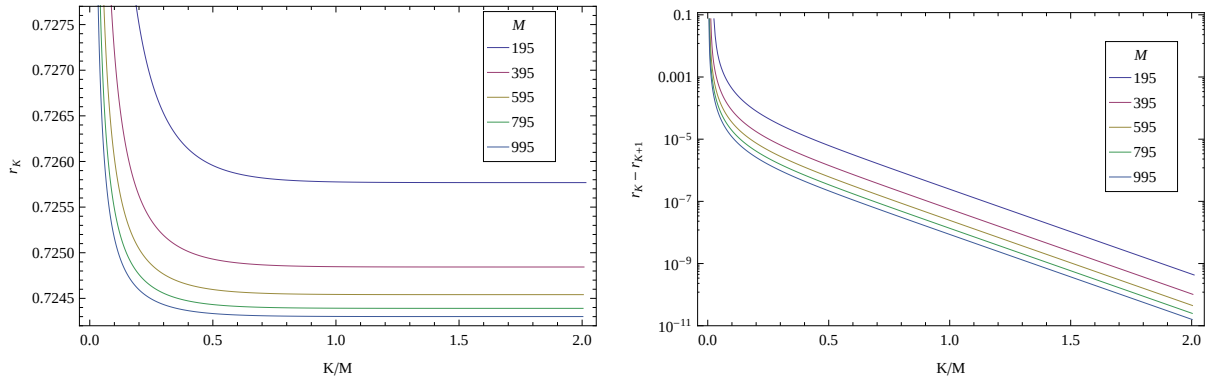

Figure 13: Linear plot and Log-linear plot of r_K and its first difference respectively, where each curve corresponds to fixed M and varying K. On the left we see that for $K \gg M$ r_K approaches a value which only depends on M, and on the right in particular that the difference of r_K from this value is proportional to $e^{-6.28K/M}$ for any M in this regime.

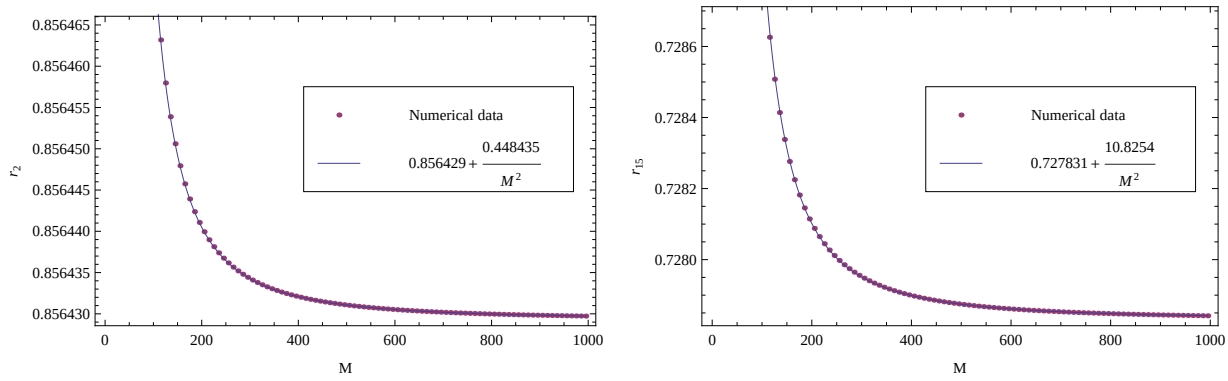

Figure 14: r_K as a function of M for $K = 2, 15$, including fits of the form (89).

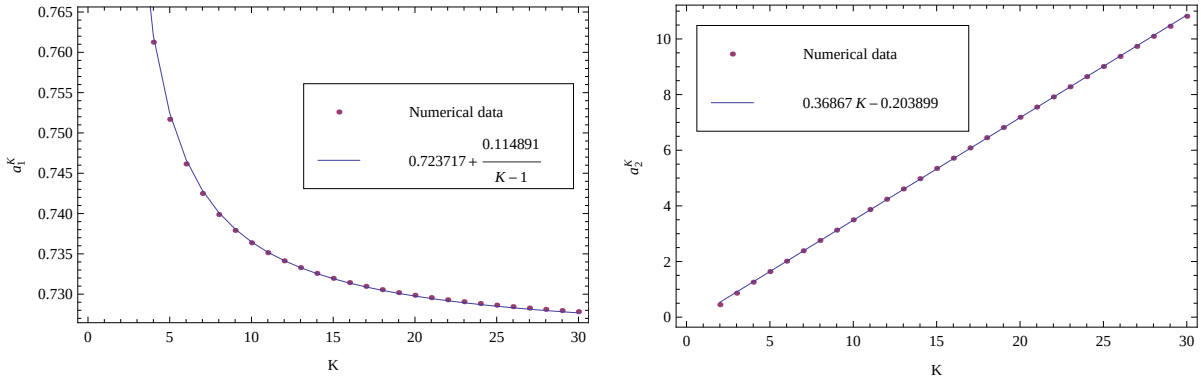

Figure 15: Values of the fitted coefficients a_1^K, a_2^K in (89) for $K = 1, \ldots, 30$ plotted against their estimates (90)-(91).

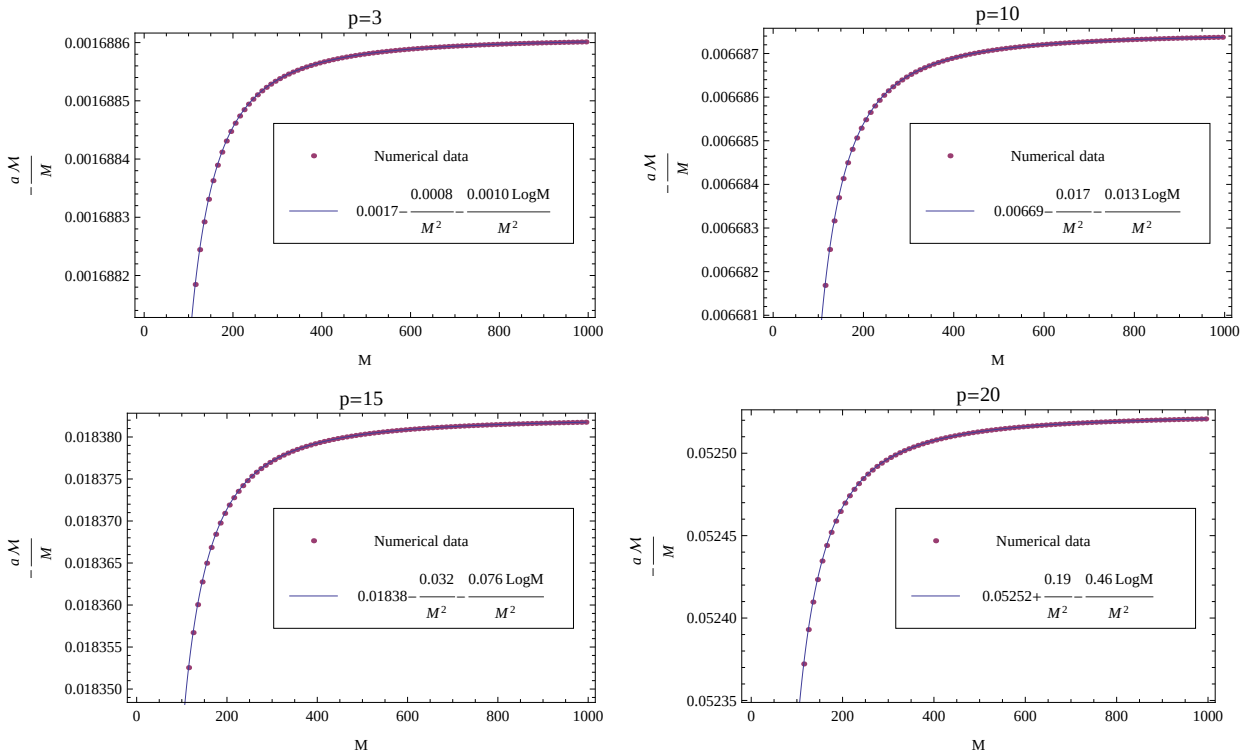

Figure 16: Rescaled zero energy amplitude for a closed string tachyon scattering off a Dp-brane for $p = 3, 10, 15, 20$ as a function of M.

In fact, it is evident that the only $1/(KM^2)$ term in the summand (88) can arise when the aforementioned p-dependent factor multiplies the $\mathcal{O}(1/M^2)$ term in δP^- (52), and given (53), our analysis constitutes a definite prediction for the relation of the $\log M/M^2$ term of the entire sum in the absence or presence of D-branes. Furthermore, the structure of r_K is such that no $1/K^2$ or K^{2n-2}/M^{2n} terms appear in the summand (88)[8], and consequently no $1/M$ terms appear in the sum, so that its expansion to next-to-next-to-leading order in M is expected to be of the the same form as in (55). Having gained this insight from the analysis of r_K and the summand, we proceed to evaluate and fit the entire zero energy amplitude (88), and find that its leading large M behavior is indeed captured by an expansion of the form

$$-\frac{a\mathcal{M}_{G,closed}}{M} = c_1 + c_2\frac{1}{M^2} + c_3\frac{\log M}{M^2}\,. \tag{92}$$

In figure 16 we compare the fit with the numerics and for sample values of p, and give for these cases the values of the p-dependent coefficients. It's worth taking a closer look at the dependence of c_3 on p in order to see the effect of the presence of D-branes on the undesirable logarithmic divergence, and also verify the prediction for its value based on the aforementioned r_K analysis. Plotting $\log(-c_3)$ as a function of $p \in [1, 25]$ (see figure 17) we

[8] $1/K^2$ would require that a_1^K has at least a linear term in K, whereas the K^l/M^{2n} terms that appear always have $l \leq n-3$ for any n.

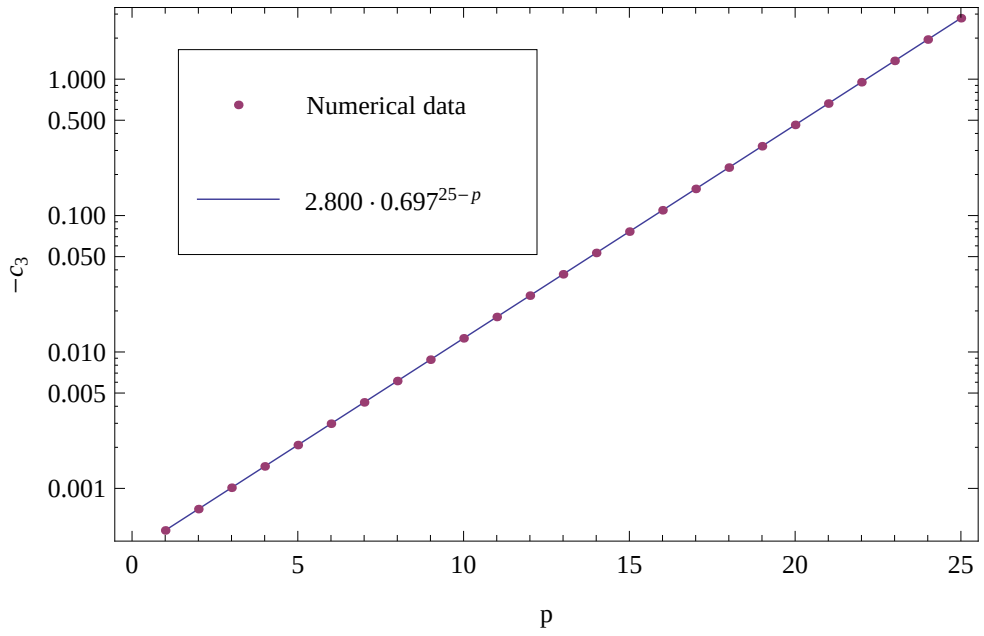

Figure 17: Log-linear plot of the $\log M/M^2$ coefficient c_3 in the large M expansion of the tachyon-Dp-brane scattering amplitude (92), as a function of p.

identify a clear linear dependence, which we can fit in order to obtain

$$c_3 = -2.800 \cdot (0.697)^{25-p} \,. \tag{93}$$

This is precisely the coefficient of the corresponding term in the closed string tachyon energy shift (56) times the factor we identified below (91). The dependence of c_3 on p shows that the presence of D-branes only softens the divergence in the sense of reducing its coefficient, but cannot remove it completely. Furthermore, these results serve as additional evidence that the existence of the divergence is solely due to the summation of the term in the summand of the closed string tachyon self-energy, which behaves as $1/K$ for small K.

Finally, let us conclude by briefly examining what changes when instead of a tachyon we have a graviton whose polarizations lie within the D-brane. We first recall that in the absence of D-branes, the summand for the graviton rescaled energy shift (58) has no $1/M^2$ term, meaning that the graviton remains massless at short distances. On the contrary here we notice that the presence of such a term in r_K (89) will carry through to the graviton summand, which can in turn be interpreted as mass generation due to the explicit breaking of Lorentz invariance by the Dirichlet boundary conditions. Although in this particular case the mass is tachyonic, generally having a mechanism for mass generation may be viewed a desirable feature, as we are ultimately interested in using open string theory to probe QCD phenomena. Thus the massless spin-1 states of the former will have to acquire a mass if they are to be put in correspondence with massive gluonic states.

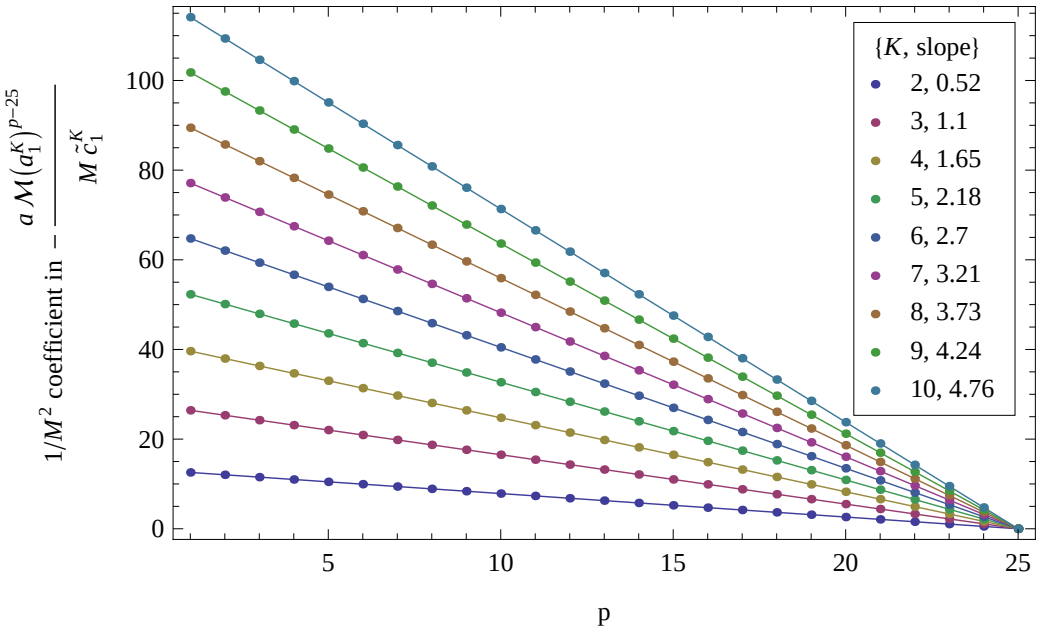

Figure 18: Ratio of the first two coefficients in the large M expansion of the summand of the tachyon-Dp-brane scattering amplitude (95), as a function of p. Each line represents the K-th term in the sum, $K = 2, \ldots, 10$, and the value of the corresponding slope is also provided in the legend.

In more detail, if our previous fits (58)-(89) have captured the M-dependence of each factor correctly, we should have

$$-\frac{a\mathcal{M}_{Graviton}}{M} = \sum_{K=2}^{\infty}[\frac{1}{2}(1+C_G^K)\delta P_K^-]\left(\sqrt{\frac{1-\eta^2}{1-\eta^{2K}}}r_K\right)^{25-p} \tag{94}$$

$$= \sum_{K=2}^{\infty}\left(\tilde{c}_1^K + \frac{\tilde{c}_2^K}{M^4} + \mathcal{O}(\frac{1}{M^5})\right)\left(a_1^K + \frac{a_2^K}{M^2} + \mathcal{O}(\frac{1}{M^3})\right)^{25-p}$$

$$= \sum_{K=2}^{\infty}\left[\tilde{c}_1^K(a_1^K)^{25-p} + (25-p)\tilde{c}_1^K(a_1^K)^{24-p}a_2^K\frac{1}{M^2} + \mathcal{O}(\frac{1}{M^3})\right]. \tag{95}$$

In particular the ratio of the second to first term should be a linear function of p with slope a_1^K/a_2^K which always becomes zero for $p = 25$, as we will now explicitly confirm. We fit the summand in (94) for $p = 1 \ldots, 25$ and $K = 2, \ldots, 10$ to inverse powers of M up to $\mathcal{O}(1/M^4)$, take the ratio of the coefficients of the first two terms and perform linear regression in terms of p for each value of K. As can be seen in figure 18, the dependence of the ratio of the coefficients on p is clearly linear with the right intercept, and comparing the slope to a_1^K/a_2^K we find that in all cases it differs less than 0.1%.

6 Discussion and Conclusion

In this article we have made a modest beginning to a critical study of the effectiveness of the worldsheet lattice, introduced in [3], for implementing a regulated bosonic string loop expansion. We have limited our analysis to the one-loop corrections to the closed string two point function in the presence of D-branes, but we plan to analyze the open string self-energy in a second paper.

A convenient way to summarize our results is to recapitulate the lightcone lattice interpretation of the divergences in the well-known covariant expression for the closed string tachyon self-energy (6):

$$-\Delta P^- \;=\; \frac{C}{2P^+}\int_0^1 \left[\frac{dq}{q^3} - 2\frac{dq}{q} + q dq\right] \tag{96}$$

The first term dq/q^3 gives a quadratic divergence, which in the covariant description is associated with the closed string tachyon disappearing into the vacuum. On the lightcone worldsheet lattice, we have seen that this divergence is interpreted as a contribution to $P^- \sim -\alpha M$, which can be cancelled by the bulk counterterm proportional to the area $M(N+1)$ of the worldsheet lattice. The only states that survive the continuum limit are those with the smallest value of α. Since only energy differences are physically significant, this shows that the quadratic divergence is physically inconsequential.

The second term dq/q gives a logarithmic divergence, associated with the disappearance of a closed string dilaton into the vacuum. This divergence can be absorbed into a renormalization of the Regge slope parameter α'. Our analysis using the worldsheet lattice has shown that this divergence shows up as a contribution to P^- behaving as $(aM)^{-1}\ln M = (T_0/P^+)\ln(P^+/aT_0)$. The noncovariance of the finite residuum was caused by a cutoff on the $K = T/a$ sum proportional to M. If the cutoff were M independent the noncovariance would disappear. We then noted that such a cutoff is naturally introduced by adding a small positive number to the boundary counterterm $B_0 \to B_0 + \epsilon$. Then the $\ln M$ is replaced by $\ln(1/\epsilon)$ which can then be covariantly absorbed in a renormalization of α', *before* the continuum limit $M \to \infty$.

This same ϵ prescription also prevents the graviton from gaining a mass in the absence of D-branes. Interestingly, in the presence of a D-brane the low energy amplitude for a graviton scattering off the D-brane, which can be thought of as a "self-energy" for a graviton propagating parallel to the D-brane, suggests a nonzero graviton "mass" in spite of the ϵ prescription. This is a consistent outcome since Lorentz invariance is broken by the Dirichlet boundary conditions. This is important in applying these ideas to large N QCD, since the closed string is supposed to model glueballs, all of which should be massive.

At a more fundamental level, we can recognize ϵ as a natural and *bona fide* physical parameter of the lightcone worldsheet system: it is simply a measure of the boundary energy $B \equiv B_0 + \epsilon$ associated with the disappearance of a link. It is also the minimum energy assigned to a free string bit. The free open string has a Lorentz invariant spectrum for only one value $B = B_0$ (or $\epsilon = 0$), but it makes sense to study the physics of the system as a

function of B (or ϵ). For sufficiently large B,

$$B > \frac{2G}{\pi}, \qquad \epsilon > \frac{2G}{\pi} - \frac{1}{2}\sinh^{-1}(1) \approx 0.1424350145, \tag{97}$$

M free string bits will have an energy greater than the ground state energy of a closed string of size M. In fact, for B this big, any system of open strings with total bit number M has energy larger than $P^-_{\rm closed,G}$. Thus for $B > 2G/\pi$, the free closed string is stable against decay into any number of open strings, and our scheme to sum planar diagrams should make good physical sense.

Dialing the value of B gives us a new tool to analyze the fate of open string tachyons in the bosonic string on the lightcone worldsheet lattice. One can attempt to simulate the sum over all patterns of missing links, as explained in the introduction, in the closed string propagator for a range of B values, and then study how the physics changes as B is gradually decreased. If the dynamics is favorable, the system should find the true vacuum with all traces of tachyons removed. Of course it is possible that the dynamics does not stabilize the theory lending weight to the prevailing opinion that the presence of tachyons of the bosonic string theory is an incurable disease which can only be cured by replacing the bosonic string with the superstring.

By introducing a D3-brane and suitable orbifold projections, it is possible to arrange the gauge boson sector of the open string to enjoy the same dynamics as gauge field theory in 4 space-time dimensions. Of course the open and closed string tachyons are still present, but they could simply be a symptom that perturbation theory is being attempted about the "wrong" vacuum. If so, analyzing the worldsheet lattice system as a function of B could provide a way to find the "right" vacuum. It will be an interesting exercise to apply these techniques to the problem of quark confinement.

Acknowledgments: This research was supported in part by the Department of Energy under Grant No. DE-FG02-97ER-41029.

A Normal Modes

A string with $P^+ = MaT_0$ is described at a fixed time by M coordinates x_i or y_i, $i = 1, \cdots M$. In this article we require several normal mode decompositions depending on the boundary conditions.

Neumann Open String

$$x_i = \frac{1}{\sqrt{M}} q_0 + \sqrt{\frac{2}{M}} \sum_{m=1}^{M-1} q_{om} \cos\frac{m\pi(i-1/2)}{M} \tag{98}$$

$$q_0 = \sqrt{\frac{1}{M}} \sum_{i=1}^{M} x_i, \qquad q_{om} = \sqrt{\frac{2}{M}} \sum_i x_i \cos\frac{m\pi(i-1/2)}{M} \tag{99}$$

Closed String (Neumann)

M odd :

$$x_i = \frac{1}{\sqrt{M}} q_0 + \sqrt{\frac{2}{M}} \sum_{m=1}^{(M-1)/2} \left[q_{cm} \cos \frac{2m\pi(i-1/2)}{M} + q_{sm} \sin \frac{2m\pi(i-1/2)}{M} \right] \quad (100)$$

M even :

$$x_i = \frac{1}{\sqrt{M}} (q_0 + q_{sM/2}(-)^i) + \sqrt{\frac{2}{M}} \sum_{m=1}^{M/2-1} \left[q_{cm} \cos \frac{2m\pi(i-1/2)}{M} + q_{sm} \sin \frac{2m\pi(i-1/2)}{M} \right] \quad (101)$$

$$q_{cm} = \sqrt{\frac{2}{M}} \sum_i x_i \cos \frac{2m\pi(i-1/2)}{M}, \qquad q_{sm} = \sqrt{\frac{2}{M}} \sum_i x_i \sin \frac{2m\pi(i-1/2)}{M} \quad (102)$$

$$q_{sM/2} = \sqrt{\frac{1}{M}} \sum_{i=1}^{M} (-)^i x_i, \qquad \text{for} \quad M \quad \text{even}, \qquad q_0 = \sqrt{\frac{1}{M}} \sum_{i=1}^{M} x_i \quad (103)$$

Dirichlet Open String

$$y_k = \sqrt{\frac{2}{M}} \sum_{m=1}^{M-1} q_{\mathrm{D}m} \sin \frac{m\pi k}{M} \quad \text{for} \quad k = 1, \cdots, M-1, \qquad y_M = q_{\mathrm{D}M} \quad (104)$$

$$q_{\mathrm{D}m} = \sqrt{\frac{2}{M}} \sum_{k=1}^{M-1} y_k \sin \frac{m\pi k}{M}, \quad 0 < m < M, \qquad q_{\mathrm{D}M} = y_M \quad (105)$$

Closed String (Dirichlet)

M odd :

$$y_i = \frac{1}{\sqrt{M}} q_0 + \sqrt{\frac{2}{M}} \sum_{m=1}^{(M-1)/2} \left[q_{cm} \cos \frac{2m\pi i}{M} + q_{sm} \sin \frac{2m\pi i}{M} \right] \quad (106)$$

M even :

$$y_i = \frac{1}{\sqrt{M}} (q_0 + q_{cM/2}(-)^i) + \sqrt{\frac{2}{M}} \sum_{m=1}^{M/2-1} \left[q_{cm} \cos \frac{2m\pi i}{M} + q_{sm} \sin \frac{2m\pi i}{M} \right] \quad (107)$$

$$q_{cm} = \sqrt{\frac{2}{M}} \sum_i y_i \cos \frac{2m\pi i}{M}, \qquad q_{sm} = \sqrt{\frac{2}{M}} \sum_i y_i \sin \frac{2m\pi i}{M} \quad (108)$$

$$q_0 = \sqrt{\frac{1}{M}} \sum_{i=1}^{M} y_i, \qquad q_{cM/2} = \sqrt{\frac{1}{M}} \sum_{i=1}^{M} (-)^i y_i, \quad (\text{for } M \text{ even}) \quad (109)$$

B Determinants

Define the normal mode frequencies of a one dimensional harmonic chain

$$\begin{aligned}
\alpha_n &\equiv 4\sin^2\frac{n\pi}{2(N+1)}, \qquad n=1,2,\ldots,N && (110)\\
\beta_n &\equiv 4\sin^2\frac{m\pi}{2M}, \qquad m=0,1,\ldots,M-1 && (111)\\
\gamma_k &\equiv 4\sin^2\frac{(k+1/2)\pi}{2K+1}, \qquad k=0,1,\ldots,K-1 && (112)\\
\delta_n &\equiv 4\sin^2\frac{m\pi}{M}, \qquad m=0,1,\ldots,M-1 && (113)
\end{aligned}$$

where $\alpha,\beta,\gamma,\delta$ are the modes of a Dirichlet-Dirichlet, Neumann-Neumann, Dirichlet-Neumann, closed chain respectively. Then we are interested in the following determinants: (see, for example [15]:

$$\begin{aligned}
D_{\rm DDDD} &= \prod_{n=1}^{N}\prod_{m=1}^{M-1}(\alpha_n+\beta_m)^{-1/2}, \qquad D_{\rm DNDN} = \prod_{n=1}^{N}\prod_{m=0}^{M-1}(\alpha_n+\beta_m)^{-1/2}\\
D_{\rm DDDN} &= \prod_{m=1}^{M-1}\prod_{k=0}^{K-1}(\beta_m+\gamma_k)^{-1/2}, \qquad D_{\rm DNNN} = \prod_{m=0}^{M-1}\prod_{k=0}^{K-1}(\beta_m+\gamma_k)^{-1/2} \qquad (114)\\
D_{\rm DD\ ring} &= \prod_{n=1}^{N}\prod_{m=0}^{M-1}(\alpha_n+\delta_m)^{-1/2}, \qquad D_{\rm ND\ ring} = \prod_{n=0}^{N-1}\prod_{m=0}^{M-1}(\gamma_n+\delta_m)^{-1/2}
\end{aligned}$$

where the subscripts denote Dirichlet (D) or Neumann (N) boundary conditions on each of the four edges of the rectangle. The cylinder determinant with Neumann boundary conditions must be defined to exclude the overall zero mode:

$$\begin{aligned}
D_{\rm NN\ ring} &\equiv \sqrt{MN}\prod_{(n,m)\neq(0,0)}(\beta_n+\delta_m)^{-1/2} = \sqrt{MN}\prod_{m=1}^{M-1}\delta_m^{-1/2}D_{\rm DD\ ring}\\
&= \sqrt{\frac{N}{M}}D_{\rm DD\ ring} \qquad (115)
\end{aligned}$$

The following product identities can be easily derived:

$$\begin{aligned}
\prod_{n=1}^{N}(\alpha_n-z) &= \frac{\sin(N+1)\kappa}{\sin\kappa}, \qquad \prod_{k=0}^{K-1}(\gamma_k-z) = \frac{\cos[(2K+1)\kappa/2]}{\cos[\kappa/2]} && (116)\\
\prod_{m=1}^{M-1}(\delta_m-z) &= \frac{\sin^2(M\kappa/2)}{\sin^2(\kappa/2)}, \qquad \prod_{m=1}^{M-1}(\beta_m-z) = \frac{\sin M\kappa}{\sin\kappa} && (117)
\end{aligned}$$

where z and κ are related by $z=4\sin^2[\kappa/2]$. Applying these identities at $z=0,\kappa=0$ shows immediately that $D_{\rm DNDN}=D_{\rm DDDD}/\sqrt{N+1}$ and $D_{\rm DNNN}=D_{\rm DDDN}$.

For convenience we collect here the expressions for the open and closed string propagators at vanishing initial and final coordinates [3]. These quantities are the determinants just discussed in their various guises. For example $\mathcal{D}^{\rm open}$ is simply related to $D_{\rm DNDN}$, with one of the products performed using the identities (117).

$$\mathcal{D}^{\rm open}(N+1) = \frac{1}{\sqrt{N+1}}\left(\frac{T_0}{2\pi}\right)^{M/2}\prod_{m=1}^{M-1}\left[\frac{\sinh(N+1)\lambda_m^o}{\sinh\lambda_m^o}\right]^{-1/2} \equiv \mathcal{D}^{\rm open}_{\rm even}\mathcal{D}^{open}_{\rm odd} \quad (118)$$

$$\mathcal{D}^{open}_{\rm odd}(N+1) = \left(\frac{T_0}{2\pi}\right)^{(M-1)/4}\prod_{m=1,{\rm odd}}^{M-1}\left[\frac{\sinh(N+1)\lambda_m^o}{\sinh\lambda_m^o}\right]^{-1/2} \quad (119)$$

$$\mathcal{D}^{closed}(N+1) = \frac{1}{\sqrt{N+1}}\left(\frac{T_0}{2\pi}\right)^{M/2}\prod_{m=1}^{M-1}\left[\frac{\sinh(N+1)\lambda_m^c}{\sinh\lambda_m^c}\right]^{-1/2} \equiv \mathcal{D}^{\rm closed}_{\rm cos}\mathcal{D}^{\rm closed}_{\rm sin} \quad (120)$$

$$\mathcal{D}^{\rm closed}_{\rm sin}(N+1) = \left(\frac{T_0}{2\pi}\right)^{(M-1)/4}\prod_{m=1}^{(M-1)/2}\left[\frac{\sinh(N+1)\lambda_m^c}{\sinh\lambda_m^c}\right]^{-1/2} \quad (121)$$

where, for simplicity, we have written these formulas assuming M is odd. If M were even, appropriate adjustments to the limits of the products must be made.

C Propagators

C.1 Neumann Open String Propagator

$$\langle N+1,\{x^f\}|0,\{x^i\}\rangle^{open} = \mathcal{D}^{open}(N+1)e^{iW_{open}} \quad (122)$$

$$iW_{open} = -\frac{T_0}{2}\Big[\frac{(q_{0,f}-q_{0,i})^2}{N+1} + \sum_{m=1}^{M-1}\sinh\lambda_m^o\left((q_{m,i}^2+q_{m,f}^2)\coth(N+1)\lambda_m^o - 2\frac{q_{m,i}q_{m,f}}{\sinh(N+1)\lambda_m^o}\right)\Big] \quad (123)$$

$$\lambda_m^o = 2\sinh^{-1}\left(\sin\frac{m\pi}{2M}\right) \quad (124)$$

Where the q_m's are the normal mode coordinates for the x's. The right side is the result of doing the integrations over all the x_i^j with $i=1,\cdots,M$ and $j=1,\cdots N$. The propagator spans $N+1$ time steps and this result corresponds to assigning half the potential energy $T_0\sum_{i=1}^{M-1}(x_{i+1}^j-x_i^j)^2/2$ to time $j=0$ and half to $j=N+1$.

C.2 Dirichlet Open String Propagator

The Dirichlet open string propagator over a time of $K=N+1$ steps is evaluated to be

$$\langle N+1,\{q^f\}|0,\{q^i\}\rangle^{\rm D} = \mathcal{D}^{\rm D}(N+1)e^{iW^{\rm D}} \quad (125)$$

where

$$iW^{\rm D} = -\frac{T_0}{2}\left[\sum_{m=1}^{M}\left((q_{{\rm D}m}^{f2}+q_{{\rm D}m}^{i2})\sinh\lambda_m^{\rm D}\coth K\lambda_m^{\rm D} - 2q_{{\rm D}m}^f q_{{\rm D}m}^i\frac{\sinh\lambda_m^{\rm D}}{\sinh K\lambda_m^{\rm D}}\right)\right] \quad (126)$$

$$\mathcal{D}^{\rm D}(N+1) = \left(\frac{T_0}{2\pi}\right)^{M/2}\prod_{m=1}^{M}\left[\frac{\sinh(N+1)\lambda_m^{\rm D}}{\sinh\lambda_m^{\rm D}}\right]^{-1/2} \quad (127)$$

$$\lambda_M^{\rm D} = 2\sinh^{-1}\sqrt{\frac{\kappa}{2}}, \qquad \lambda_m^{\rm D}=\lambda_m^o = 2\sinh^{-1}\sin\frac{m\pi}{2M}, \quad m=1,\cdots M-1 \quad (128)$$

We recall that the above expressions give the the result of integrating over all the variables y_i^j, for $j=1,\cdots,N$, with half the potential energy assigned to $j=0,N+1$, which is consistent with the closure requirement.

C.3 Closed String Propagator

$$\langle N+1,\{x^f\}|0,\{x^i\}\rangle^{closed} = \mathcal{D}^{closed}(N+1)e^{iW_{closed}} \quad (129)$$

$$iW_{closed} = -\frac{T_0}{2}\Big[\frac{(q_{0,f}-q_{0,i})^2}{N+1} \sum_{m=1}^{M-1}\sinh\lambda_m^c\left((q_{m,i}^2+q_{m,f}^2)\coth(N+1)\lambda_m^c - 2\frac{q_{m,i}q_{m,f}}{\sinh(N+1)\lambda_m^c}\right)\Big] \quad (130)$$

$$\lambda_m^c = 2\sinh^{-1}\left(\sin\frac{m\pi}{M}\right) \quad (131)$$

Where the q_m's are the normal mode coordinates for the x's. When we divide the closed string normal modes into sine and cosine modes, we arbitrarily call the $m>M/2$ modes sine modes and the $m<M/2$ modes cosine modes. When M is even, the $M/2$ mode is not doubled. The right side is the result of doing the integrations over all the x_i^j with $i=1,\cdots,M$ and $j=1,\cdots N$. The propagator spans $N+1$ time steps and this result corresponds to assigning half the potential energy $T_0\sum_{i=1}^{M}(x_{i+1}^j-x_i^j)^2/2$ to time $j=0$ and half to $j=N+1$. In sums like these it is understood that $x_{M+1}^j\equiv x_1^j$. Whenever we concatenate at a time j propagators with different numbers of missing links, we will understand that we *add* terms $T_0(\Delta x)^2/4$ in the exponent so that the potential assigned to time j is that of the system with the least number of missing links. For example, the concatenation of an open string propagator with a closed string propagator entails the addition of $T_0(x_M^j-x_1^j)^2/4$ to the exponent.

Finally, we resolve the zero mode dependence of the propagators in momentum space

$$\int\frac{dp}{2\pi}e^{-p^2T/2P^+}e^{i(x_f^{CM}-x_i^{CM})p} = \sqrt{\frac{P^+}{2\pi T}}e^{-P^+(x_f^{CM}-x_i^{CM})^2/2T}$$

$$= \sqrt{\frac{MT_0}{2\pi(N+1)}}e^{-MT_0(x_f^{CM}-x_i^{CM})^2/2(N+1)}$$

$$\int \frac{dp}{2\pi} e^{-p^2 T/2P^+} e^{i(x_f^{CM} - x_i^{CM})p} = \sqrt{\frac{MT_0}{2\pi(N+1)}} e^{-T_0(q_{0,f}-q_{0,i})^2/2(N+1)} , \tag{132}$$

where $x^{CM} \equiv \sum_k x_k/M = q_0/\sqrt{M}$ is the center of mass coordinate. From this we see that in extracting eigenstate amplitudes from propagators defined with Dirichlet conditions on initial and final states, we must not include the factors $\sqrt{MT_0/2\pi(N+1)}$.

D Overlap Formulas

Neumann Open-Closed

$$q_{om} = \begin{cases} q_{cm/2} & m \text{ even} \\ \frac{2}{M} \sum_{m'=1}^{(M-1)/2} q_{sm'} U_{mm'} & m \text{ odd} \end{cases} \tag{133}$$

$$U_{mm'} = \frac{\sin(m'\pi/M)\cos(m\pi/2M)}{\sin^2(m'\pi/M) - \sin^2(m\pi/2M)} \tag{134}$$

Dirichlet Open-Closed

$$q_{\mathrm{D}M} = \frac{1}{\sqrt{M}} q_0 + \sqrt{\frac{2}{M}} \sum_{m'=1}^{(M-1)/2} q_{cm'} \equiv \sqrt{\frac{2}{M}} \sum_{m'=0}^{(M-1)/2} q_{cm'} \tag{135}$$

$$q_{\mathrm{D}m} = q_{sm/2}, \qquad \text{for} \quad m \text{ even} \tag{136}$$

$$\begin{aligned} q_{\mathrm{D}m} &= \frac{\sqrt{2}}{M} q_0 \sum_{k=1}^{M-1} \sin\frac{m\pi k}{M} + \frac{2}{M} \sum_{m'=1}^{(M-1)/2} q_{cm'} \sum_{k=1}^{M-1} \sin\frac{m\pi k}{M} \cos\frac{2m'\pi k}{M} \\ &\equiv \frac{2}{M} \sum_{m'=0}^{(M-1)/2} q_{cm'} \sum_{k=1}^{M-1} \sin\frac{m\pi k}{M} \cos\frac{2m'\pi k}{M} \end{aligned} \tag{137}$$

where, for convenience, we have defined $q_{c0} \equiv q_0/\sqrt{2}$. The sum over k is easily done

$$\sum_{k=1}^{M-1} \sin\frac{m\pi k}{M} \cos\frac{2m'\pi k}{M} = \frac{\delta_{m \text{ odd}}}{2} \frac{\sin(m\pi/M)}{\sin^2(m\pi/2M) - \sin^2(m'\pi/M)} \equiv \delta_{m \text{ odd}} U^{\mathrm{D}}_{mm'} \tag{138}$$

for odd $m < M$. We can unify the treatment of the $m = M$ mode by defining $U^{\mathrm{D}}_{Mm'} = \sqrt{M/2}$ for $m' = 0, 1, \cdots, (M-1)/2$:

$$q_{\mathrm{D}m} = \begin{cases} q_{sm/2} & \text{for } m \text{ even} \\ \frac{2}{M} \sum_{m'=0}^{(M-1)/2} q_{cm'} U^{\mathrm{D}}_{mm'} & \text{for } m \text{ odd} \end{cases} \tag{139}$$

Open-2 Open

$$q_0^{(1)} = \sqrt{\frac{M_1}{M}}\, q_0 + \sqrt{\frac{2}{MM_1}} \sum_{m'=1}^{M-1} q_{m'} U^{(1)}_{m'0}, \qquad q_m^{(1)} = \frac{2}{\sqrt{MM_1}} \sum_{m'=1}^{M-1} q_{m'} U^{(1)}_{m'm} \tag{140}$$

$$q_0^{(2)} = \sqrt{\frac{M_2}{M}}\, q_0 + \sqrt{\frac{2}{MM_2}} \sum_{m'=1}^{M-1} q_{m'} U^{(2)}_{m'0}, \qquad q_m^{(2)} = \frac{2}{\sqrt{MM_2}} \sum_{m'=1}^{M-1} q_{m'} U^{(2)}_{m'm} \tag{141}$$

$$\begin{aligned} U^{(1)}_{m'm} &= \sum_{i=1}^{M_1} \cos\frac{m'\pi}{M}\left(i-\frac{1}{2}\right) \cos\frac{m\pi}{M_1}\left(i-\frac{1}{2}\right) \\ &= \frac{(-)^m}{2} \frac{\sin(m'\pi M_1/M)\sin(m'\pi/2M)\cos(m\pi/2M_1)}{\sin^2(m'\pi/2M)-\sin^2(m\pi/2M_1)} \end{aligned} \tag{142}$$

$$\begin{aligned} U^{(2)}_{m'm} &= \sum_{i=1+M_1}^{M} \cos\frac{m'\pi}{M}\left(i-\frac{1}{2}\right) \cos\frac{m\pi}{M_2}\left(i-M_1-\frac{1}{2}\right) \\ &= -\frac{1}{2} \frac{\sin(m'\pi M_1/M)\sin(m'\pi/2M)\cos(m\pi/2M_2)}{\sin^2(m'\pi/2M)-\sin^2(m\pi/2M_2)} \end{aligned} \tag{143}$$

and we note the identity $q_0^{(1)}\sqrt{M_1}+q_0^{(2)}\sqrt{M_2} = q_0\sqrt{M}$, as expected from the fact that $q_0/\sqrt{M}$ is the center of momentum of the open string.

We can also express the q's in terms of the $q^{(1)}, q^{(2)}$'s:

$$q_0 = q_0^{(1)}\sqrt{\frac{M_1}{M}} + q_0^{(2)}\sqrt{\frac{M_2}{M}} \tag{144}$$

$$\begin{aligned} q_{m'} &= \sqrt{\frac{2}{MM_1}}\left(q_0^{(1)} U^{(1)}_{m'0} + \sqrt{2}\sum_{m=1}^{M_1-1} q_m^{(1)} U^{(1)}_{m'm}\right) \\ &\quad + \sqrt{\frac{2}{MM_2}}\left(q_0^{(2)} U^{(2)}_{m'0} + \sqrt{2}\sum_{m=1}^{M_2-1} q_m^{(2)} U^{(2)}_{m'm}\right) \end{aligned} \tag{145}$$

E Robustness of numerical results

In this appendix, we perform additional tests which verify the correctness of our numerical results, within the stated accuracy. In particular, we recalculate δP_K^- with more significant digits[9] for indicative values of M and K, and examine the improvement in its accuracy.

We will use the difference in δP_K^- between the calculations with different number of significant digits, $\Delta(\delta P_K^-)$, as a measure of our numeric error. We first notice that $\Delta(\delta P_K^-)$ decreases almost exponentially when K increases for fixed M, as can be seen in the example of figure 19.

The decrease is so rapid that we can clearly consider the error of the $K = 1$ term as the error of the entire sum, giving the rescaled ground state energy shift $\Delta P^-_{G,closed}$ in (51).

[9] In particular, we now keep 20 significant digits compared to the 16 we had initially.

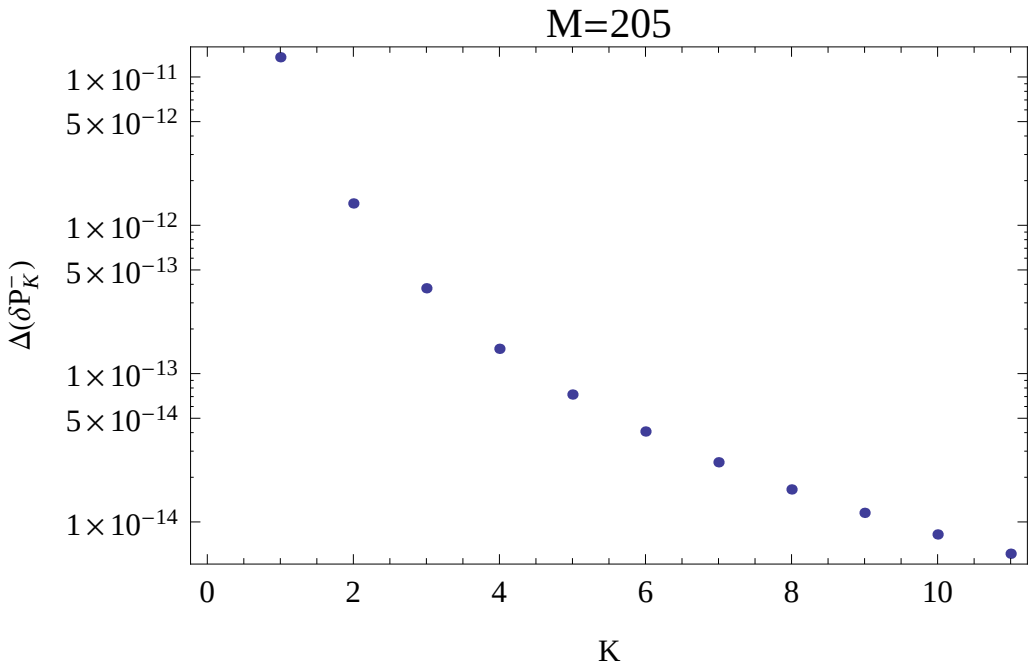

Figure 19: Log-linear plot of the change in accuracy $\Delta(\delta P_K^-)$ as a function of K for $M = 205$.

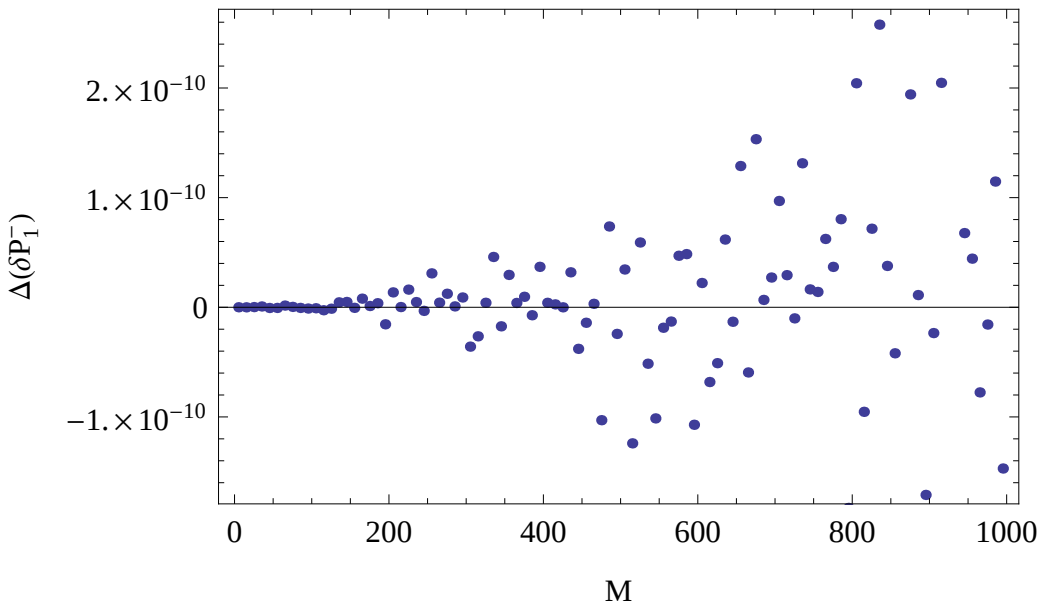

Figure 20: Plot of the leading change in accuracy $\Delta(\delta P_1^-)$ as a function of M.

Fortunately, in this case we know the exact value $\delta P_1^- = 1$ for any M, allowing us to also obtain the exact deviation of our numerical results from it, which we present in figure 20. We first notice that the deviations are centered around zero, implying that no systematic error that offsets the value of δP_1^- is present. Furthermore, it is evident that the deviation increases with M, and for the range $M \in [195, 995]$ we have based our fits on, in lies between $10^{-11} - 10^{-10}$.

Let us now compare this with the error in the fit for $\Delta P^-_{G,closed}$ (55) as a result of the uncertainty in the coefficients (56),

$$\Delta c_1 \sim 10^{-9}\,, \quad \Delta\Big(\frac{c_2}{M^2}\Big) \sim 10^{-8}\,, \quad \Delta\Big(\frac{c_3 \log M}{M^2}\Big) \sim 10^{-8} \text{ for } M \sim 10^3\,, \tag{146}$$

where we estimated the smallest possible contribution of the last two terms by replacing M with roughly the largest value we used in our numerical analysis. Clearly these uncertainties are at least one order of magnitude larger than the errors due to our choice for the number of significant digits, so the effect of the latter on the determined values for the coefficients c_i will be negligible. This successfully completes the investigation of the robustness of our numerical results.

References

[1] J. M. Maldacena, Adv. Theor. Math. Phys. **2** (1998) 231 [Int. J. Theor. Phys. **38** (1999) 1113] [hep-th/9711200].

[2] G. 't Hooft, *Nucl. Phys.* **B72** (1974) 461.

[3] R. Giles and C. B. Thorn, Phys. Rev. D **16** (1977) 366.

[4] P. Goddard, C. Rebbi, C. B. Thorn, Nuovo Cim. **A12** (1972) 425-441.

[5] P. Goddard, J. Goldstone, C. Rebbi and C. B. Thorn, Nucl. Phys. B **56** (1973) 109.

[6] S. Mandelstam, Nucl. Phys. B **64** (1973) 205. Nucl. Phys. B **69** (1974) 77.

[7] K. Bardakci and C. B. Thorn, Nucl. Phys. B **626** (2002) 287 [arXiv:hep-th/0110301]; C. B. Thorn, Nucl. Phys. B **637** (2002) 272 [Erratum-ibid. B **648** (2003) 457] [arXiv:hep-th/0203167]; S. Gudmundsson, C. B. Thorn and T. A. Tran, Nucl. Phys. B **649** (2003) 3 [arXiv:hep-th/0209102].

[8] D. Chakrabarti, J. Qiu and C. B. Thorn, Phys. Rev. D **72** (2005) 065022 [arXiv:hep-th/0507280]; D. Chakrabarti, J. Qiu and C. B. Thorn, Phys. Rev. D **74** (2006) 045018 [Erratum-ibid. D **76** (2007) 089901] [arXiv:hep-th/0602026].

[9] K. Johnson, "Quantum Electrodynamics," in *The 1964 Brandeis Summer Institute in Theoretical Physics, Volume 2: Lectures on Particles and Quantum Field Theory*, Edited by S. Deser, Prentice-Hall, 1965.

[10] M. B. Green, E. Witten, and J. H. Schwarz, "Superstring Theory: Volume 2", Cambridge University Press,1988.

[11] M. Kac, Am. Math. Mon. **73** (1966) 1. H. P. McKean and I. M. Singer, J. Diff. Geom. **1** (1967) 43. O. Alvarez, Nucl. Phys. **B216** (1983) 125.

[12] S. Mandelstam, Lectures at the Workshop on Unified String Theories, 29 July-16 August 1985, Institute for Theoretical Physics, University of Santa Barbara, Santa Barbara CA, published in *Unified String Theories*, Ed. M.Green and D. Gross, World Scientific, 1986.

[13] J. Dai, R. G. Leigh and J. Polchinski, Mod. Phys. Lett. A **4** (1989) 2073.

[14] C. B. Thorn, Phys. Rev. D **80** (2009) 086010 [arXiv:0906.3742 [hep-th]].

[15] C. B. Thorn, "Determinants for the Lightcone Worldsheet," arXiv:1205.5815 [hep-th].